astro8405

An Introduction to the

Cosmic Microwave Background

Kaustuv Basu

kbasu@uni-bonn.de

eCampus | Lernplattform der Universität Bonn

astro8405: The Cosmic Microwave Background

Aktionen

This course intends to give you a modern and up-to-date introduction to the science and experimental techniques relating to the Cosmic Microwave Background. No prior knowledge of cosmology is necessary, your prerequisite are a basic understanding of electrodynamics and thermal physics and some familiarity with Python programming.

Lecture 13:

Sunyaev-Zeldovich Effect

(Part II)

Thermal SZ effect summary

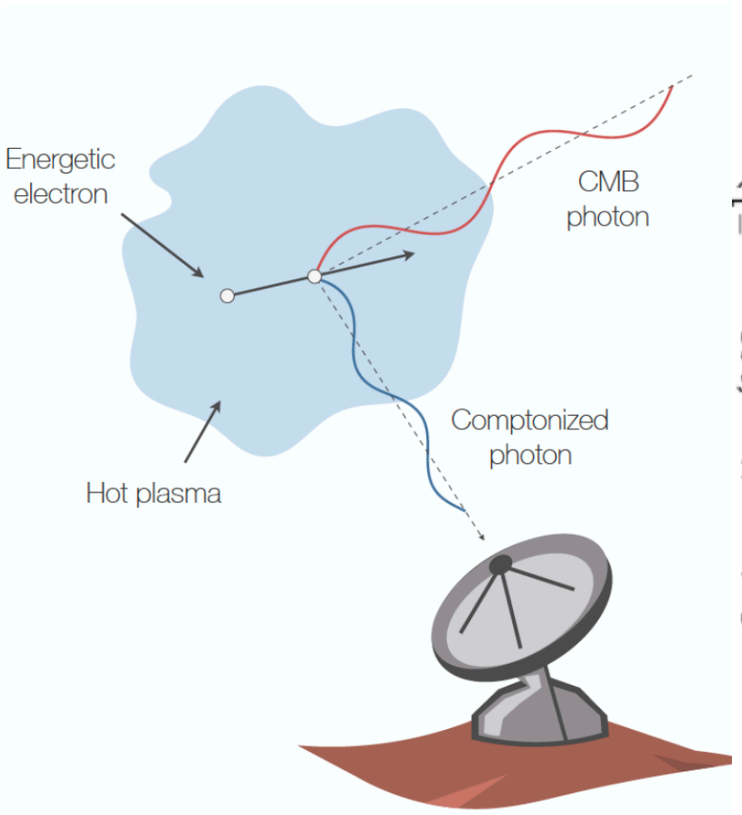

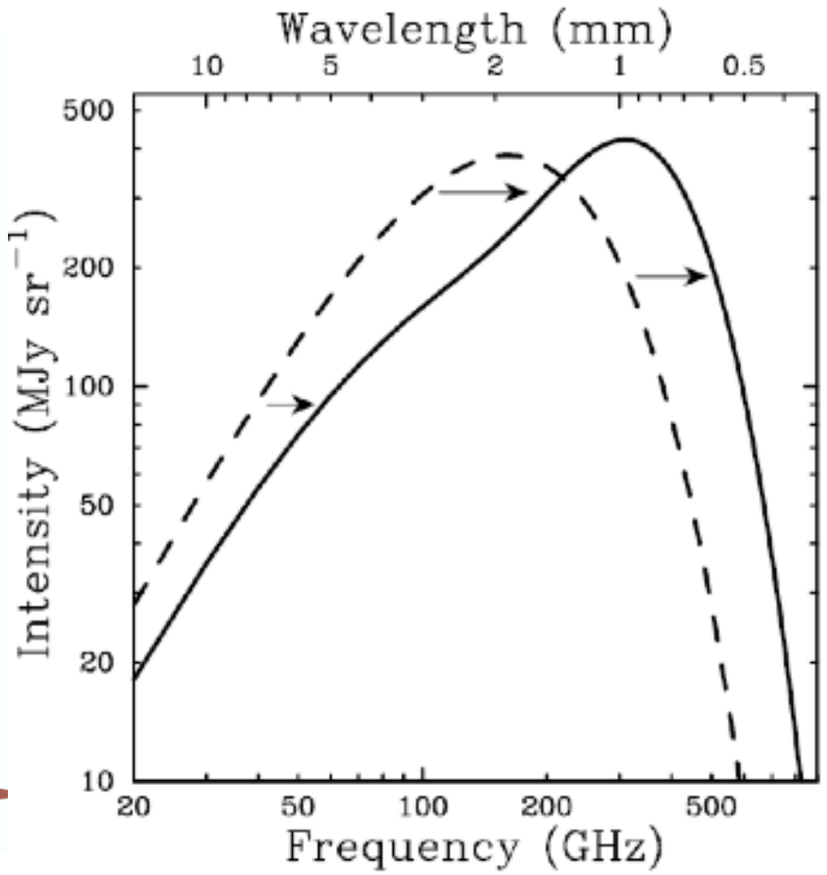

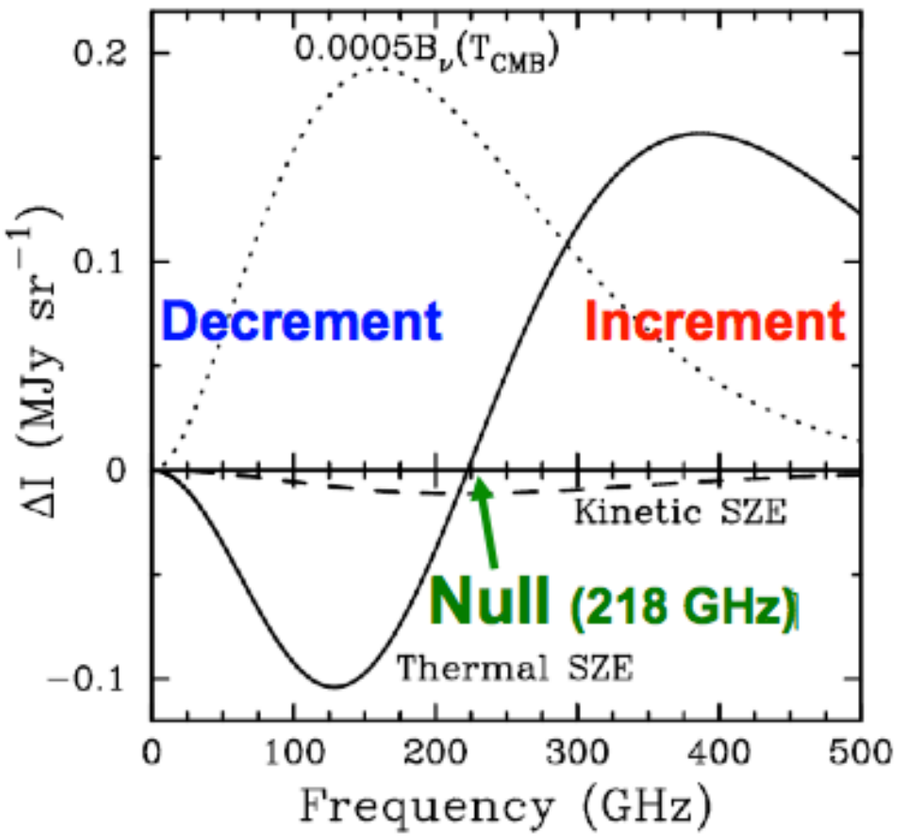

$$y \equiv \int \frac{k_\mathrm{B} T_\mathrm{e}}{m_\mathrm{e} c^2}\, \mathrm{d}\tau_\mathrm{e} = \int \frac{k_\mathrm{B} T_\mathrm{e}}{m_\mathrm{e} c^2}\, n_\mathrm{e} \sigma_\mathrm{T} \mathrm{d}l = \frac{\sigma_\mathrm{T}}{m_\mathrm{e} c^2} \int P_\mathrm{e}\, \mathrm{d}l.$$

$$\Delta I_\nu \approx I_0\, y \frac{x^4 \mathrm{e}^x}{(\mathrm{e}^x - 1)^2} \left(x \frac{\mathrm{e}^x + 1}{\mathrm{e}^x - 1} - 4 \right) \equiv I_0\, y\, g(x) \qquad \frac{\Delta T_\mathrm{CMB}}{T_\mathrm{CMB}} \approx y \left(x \frac{\mathrm{e}^x + 1}{\mathrm{e}^x - 1} - 4 \right) = y\, f(x).$$

Kinematic SZ effect summary

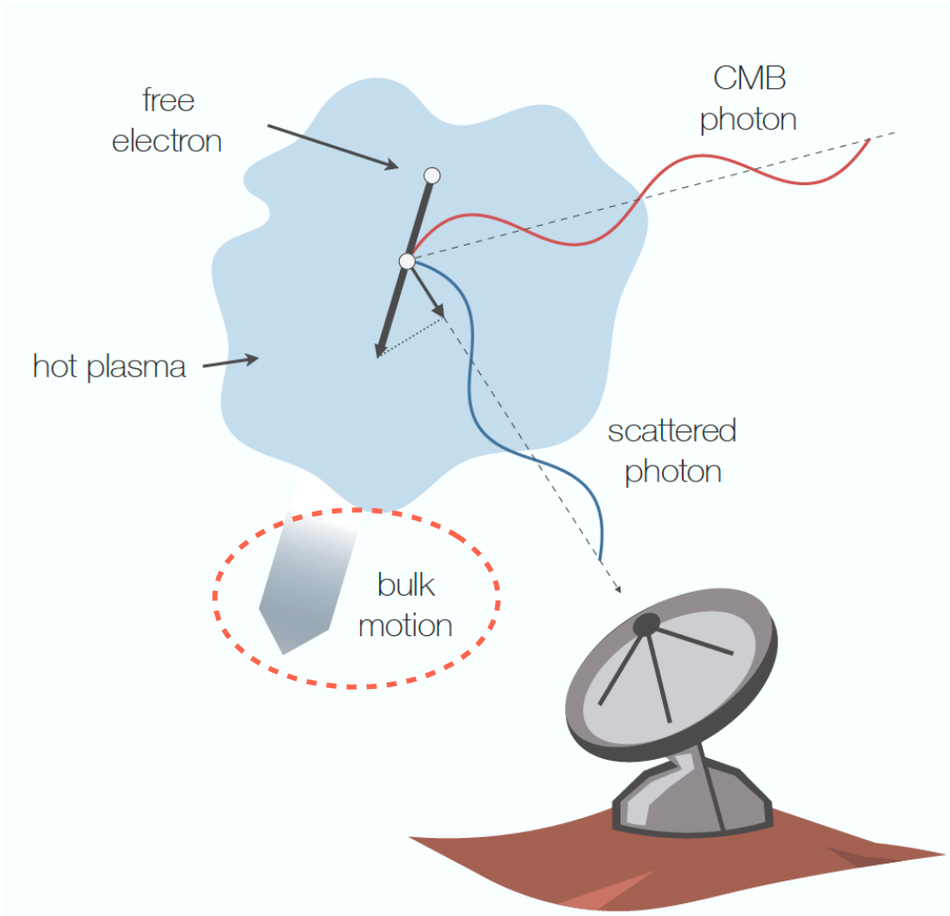

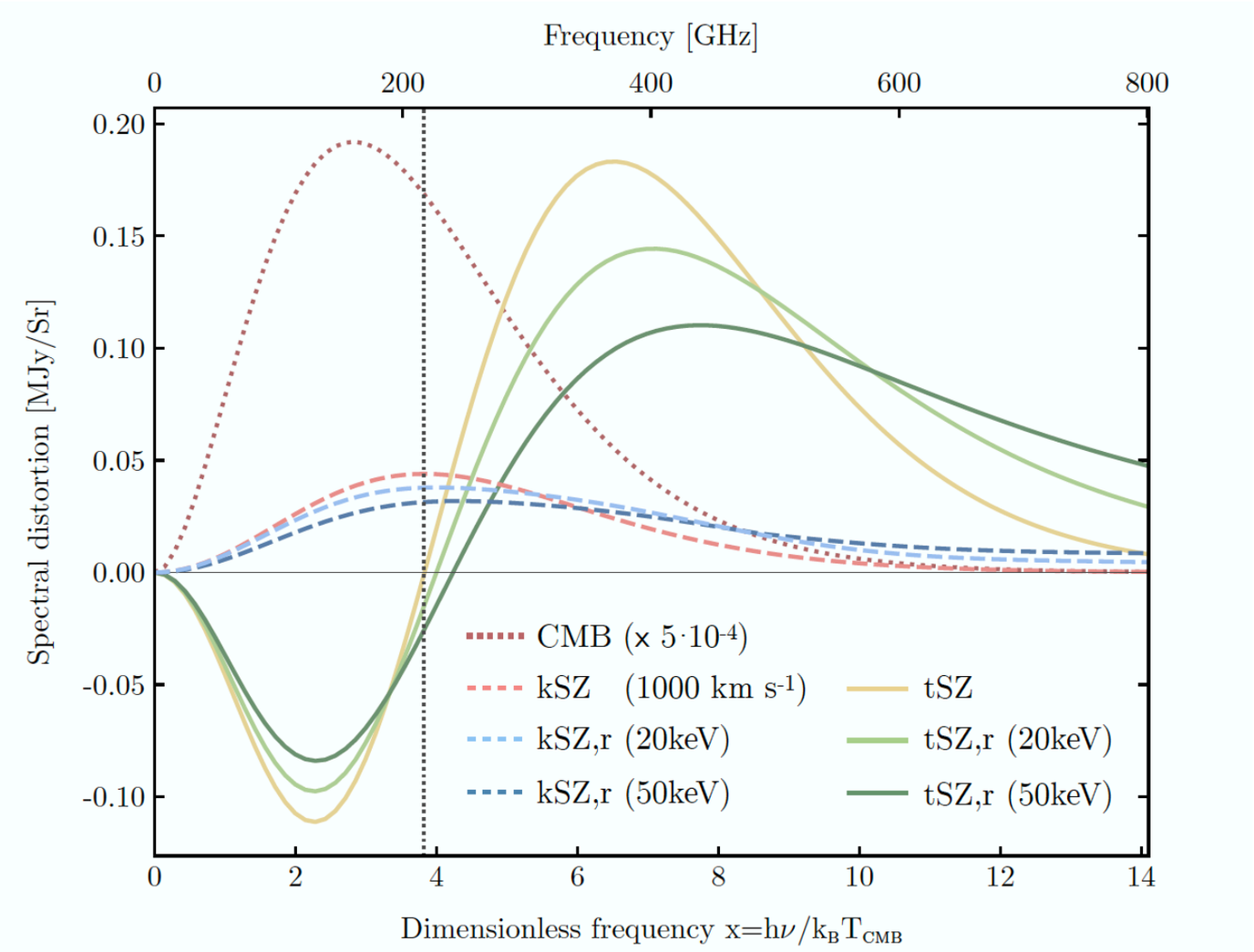

$$\frac{\Delta T_{\rm CMB}}{T_{\rm CMB}} \approx -\int \sigma_{\rm T} n_{\rm e}\, \boldsymbol{n}\cdot\boldsymbol{\beta}_{\rm p}\, {\rm d}l = -\int \boldsymbol{n}\cdot\boldsymbol{\beta}_{\rm p}\, {\rm d}\tau_{\rm e} \equiv -y_{\rm kSZ}$$

$$\Delta I_\nu \approx -I_0 \frac{x^4 {\rm e}^x}{({\rm e}^x-1)^2}\, y_{\rm kSZ}$$

The first four SZE discovered galaxy clusters

unfiltered map (with CMB)

filtered detection maps

null maps

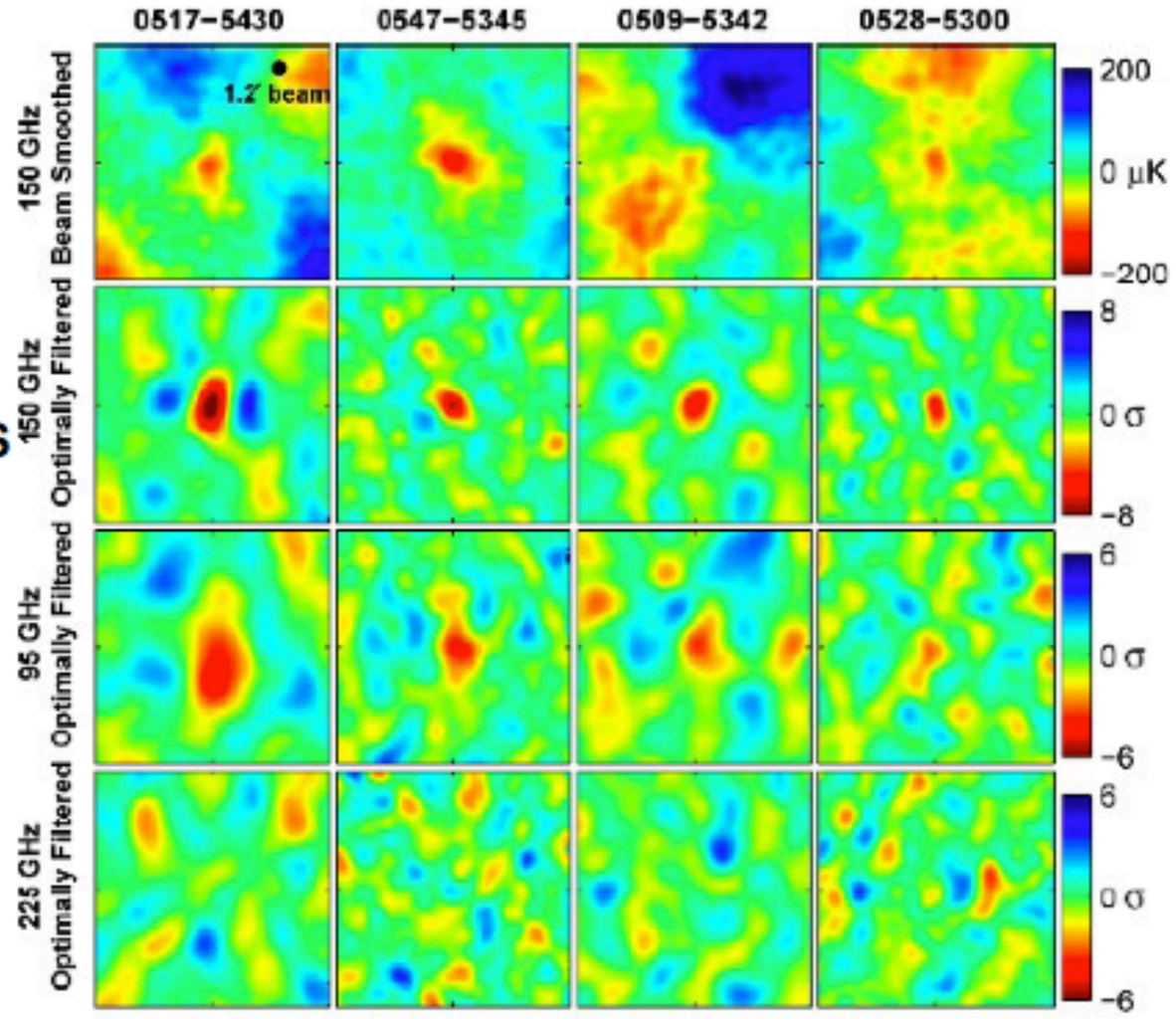

20’x20’ field-of-view

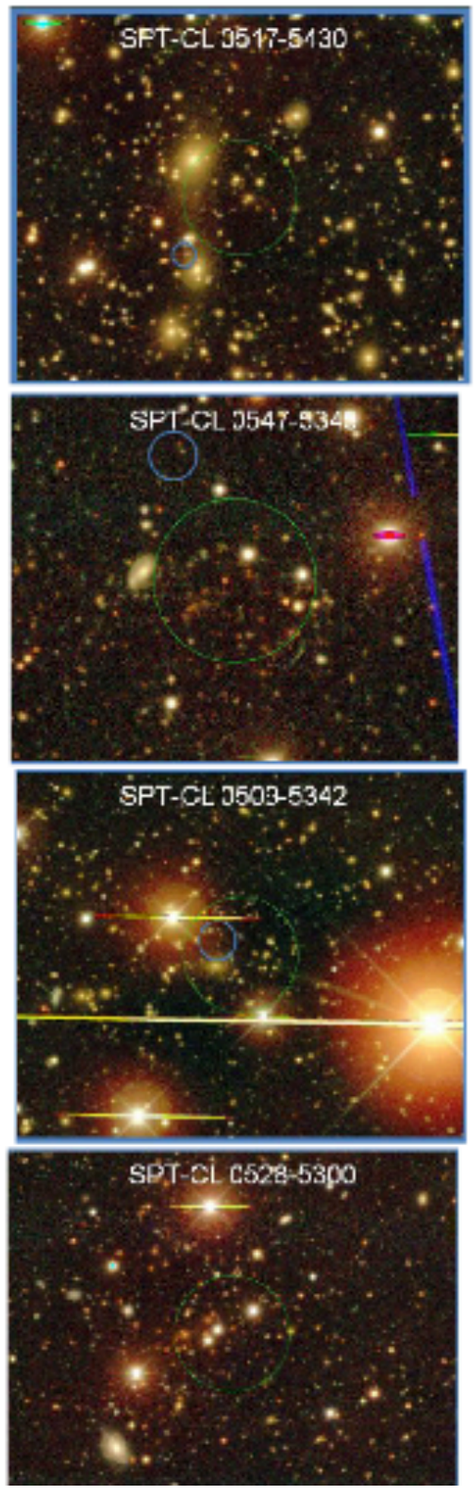

Source: Staniszewski et al. 2009

Then, in six years (Planck, SPT, ACT)

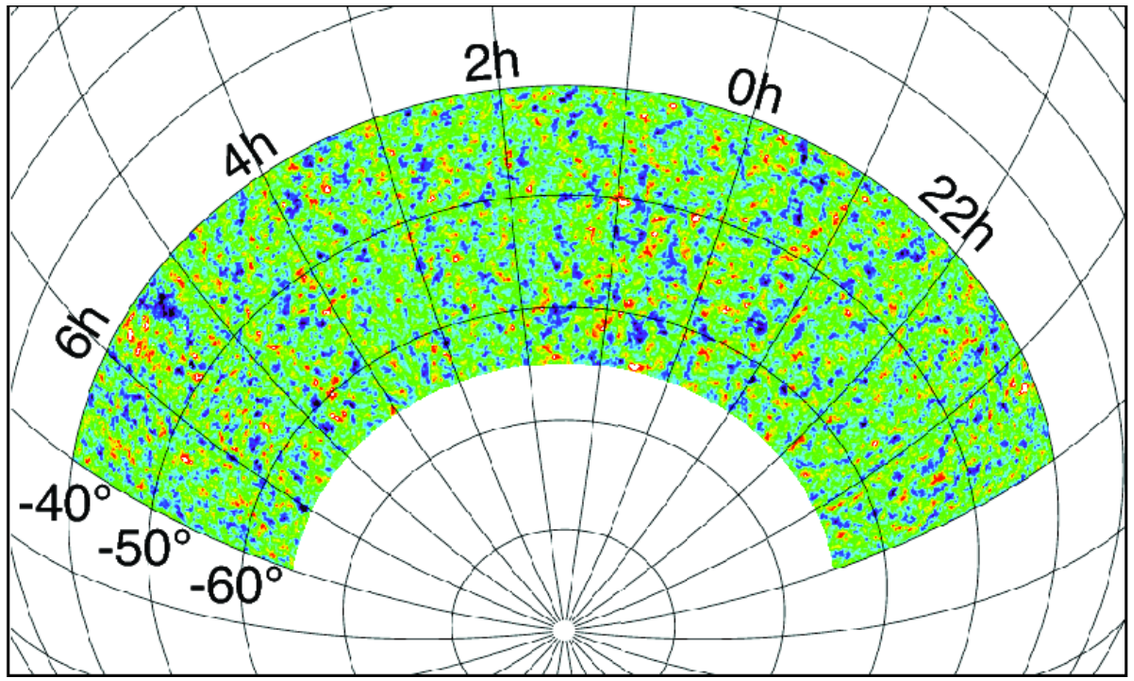

By 2015, the number of galaxy clusters detected by the SZ effect was over 2000. Planck 2015 catalog listed roughly 1600 clusters, and the SPT and ACT experiments reported over 500 clusters each from a smaller fraction of the sky.

Nearly 700 confirmed galaxy clusters from the SPT 2500 deg^2 field (Bleem et al. 2015)

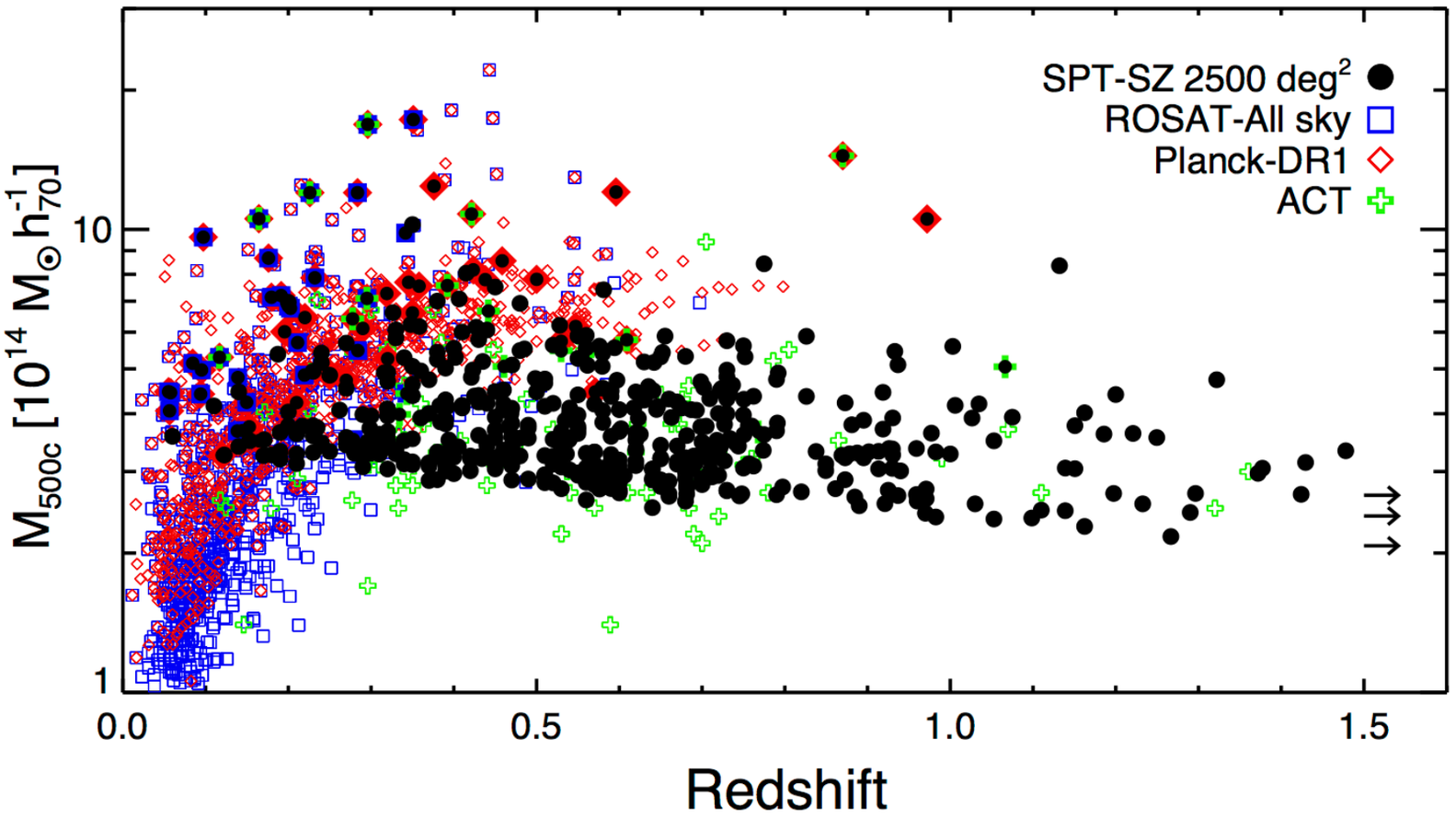

State-of-the-art: ACT (2020) results

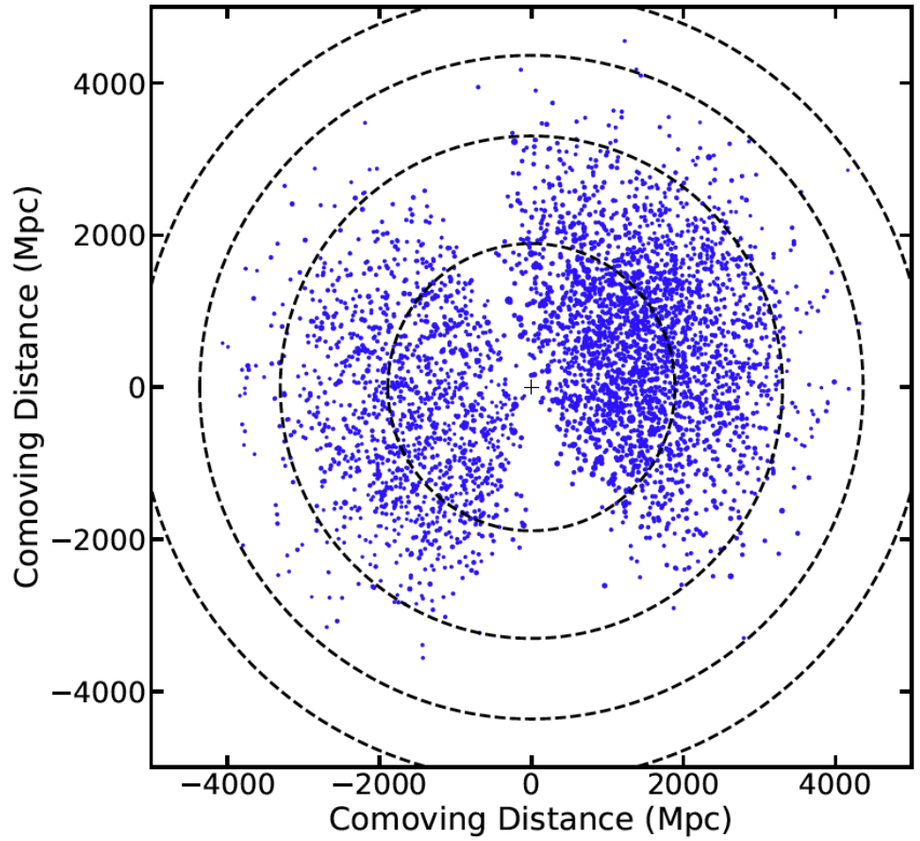

4000+ clusters
(Hilton+ 2020)

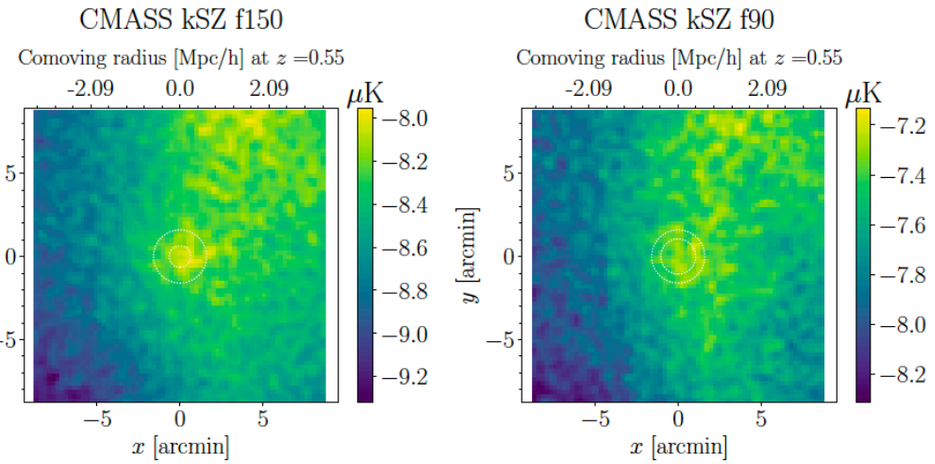

In low-mass clusters,
kSZ ~ tSZ
($v_r/c \sim kT/mc^2$)

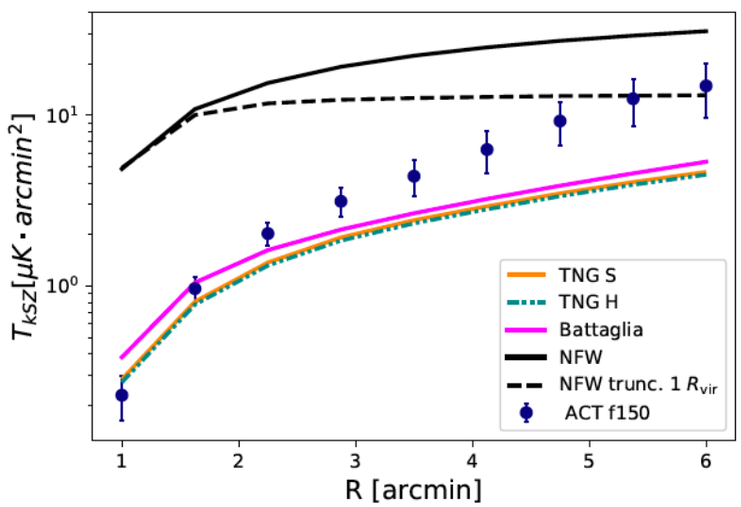

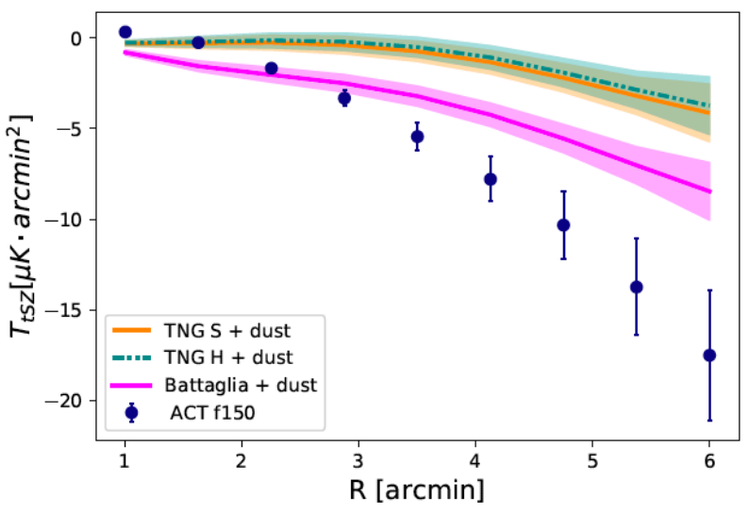

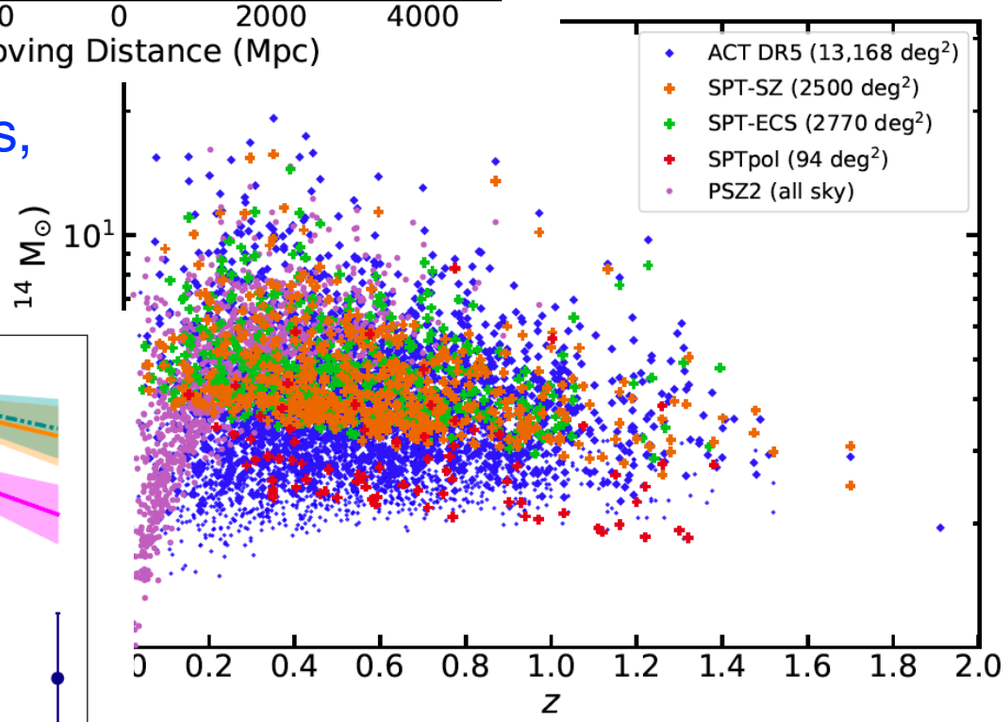

Halo thermodynamic modelling
(Schaan+, Amodeo+ 2020)

Redshift-independence of the SZ effect

Sine the SZ effect is a scattering of the background CMB photons, the effect of the cosmic expansion is the same on both the scattered and un-scattered photons. In other words, the signal is independent of redshift!

Hence if you can resolve the cluster, the total flux density within the telescope beam remains constant no matter the distance of the cluster, provided the intrinsic property of the cluster remains the same.

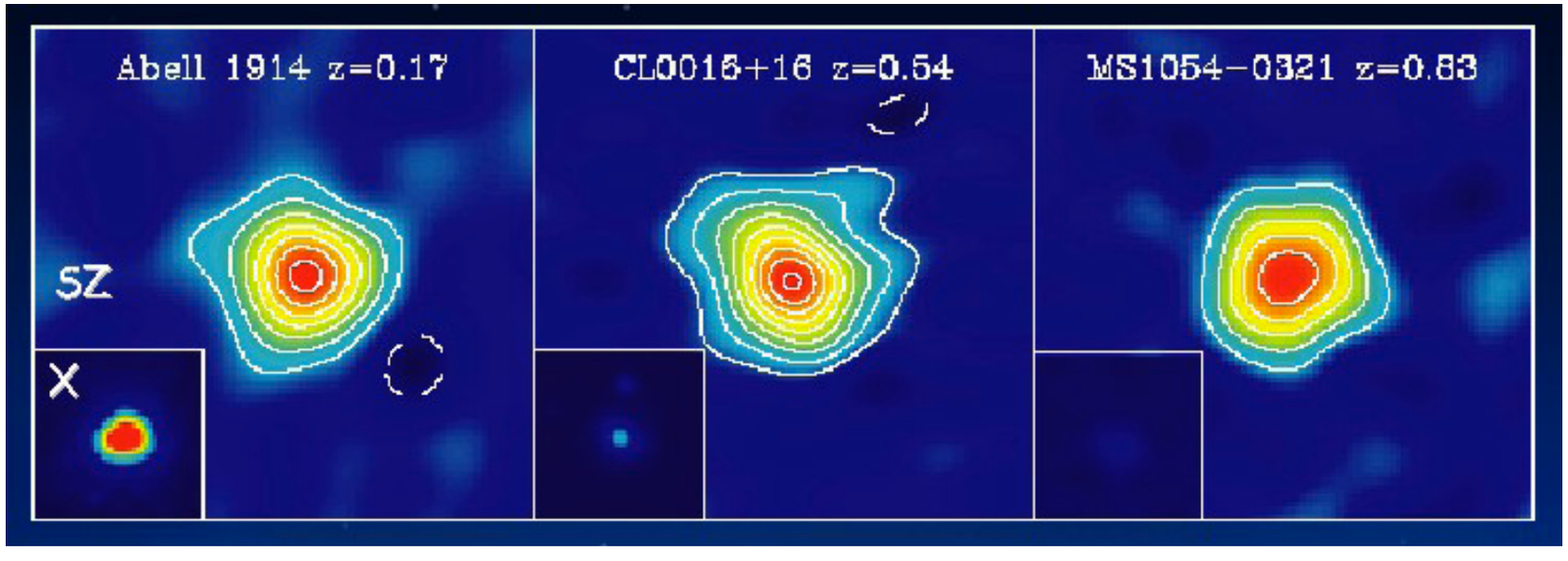

$$\Delta S_\nu = \int \Delta I_\nu \, d\Omega \propto \frac{\int n_e T_e \, dV}{D_A^2} \propto \frac{f_{\rm gas} M_{\rm tot} T_e}{D_A^2}$$

Carlstrom, Holder, and Reese (2002)

“Beam dilution” of the SZ effect

If the instrument beam is larger than the cluster, then the flux difference generated by the SZ effect gets weaker, as the cluster is more distant and hence smaller in angular diameter (think of a surface with uniform brightness getting smaller). This causes a redshift-dependent selection for some SZ experiments, like Planck (upper figure on right).

For Ground-based experiments with ~1 arcmin beam size, like SPT, this is perfectly matched with typical cluster size, and clusters at higher redshifts do not get significantly smaller. In fact, the mass threshold goes down slightly, as the clusters are actually denser and hotter (hence more SZ-bright) at high-z.

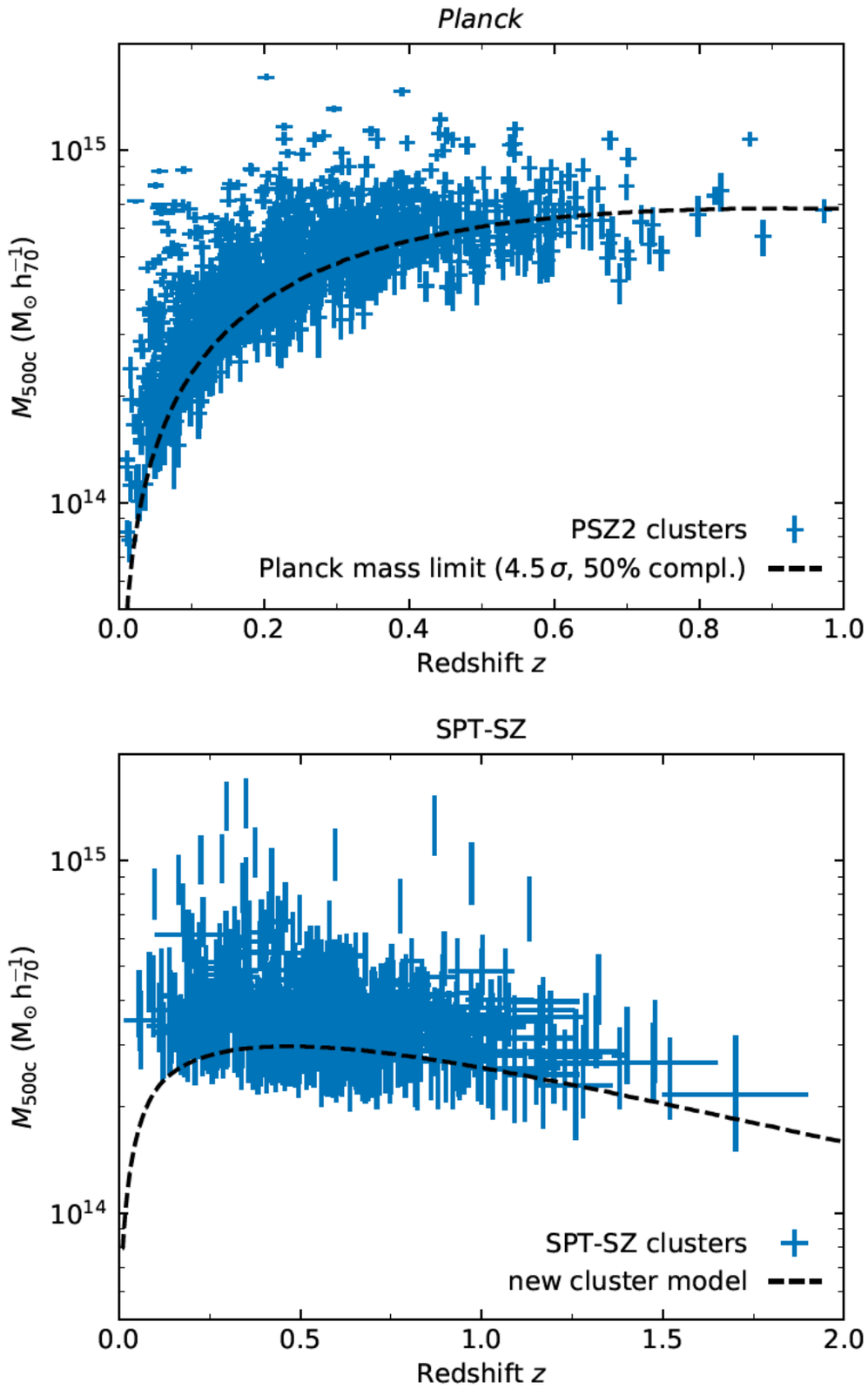

The Planck clusters from 2015

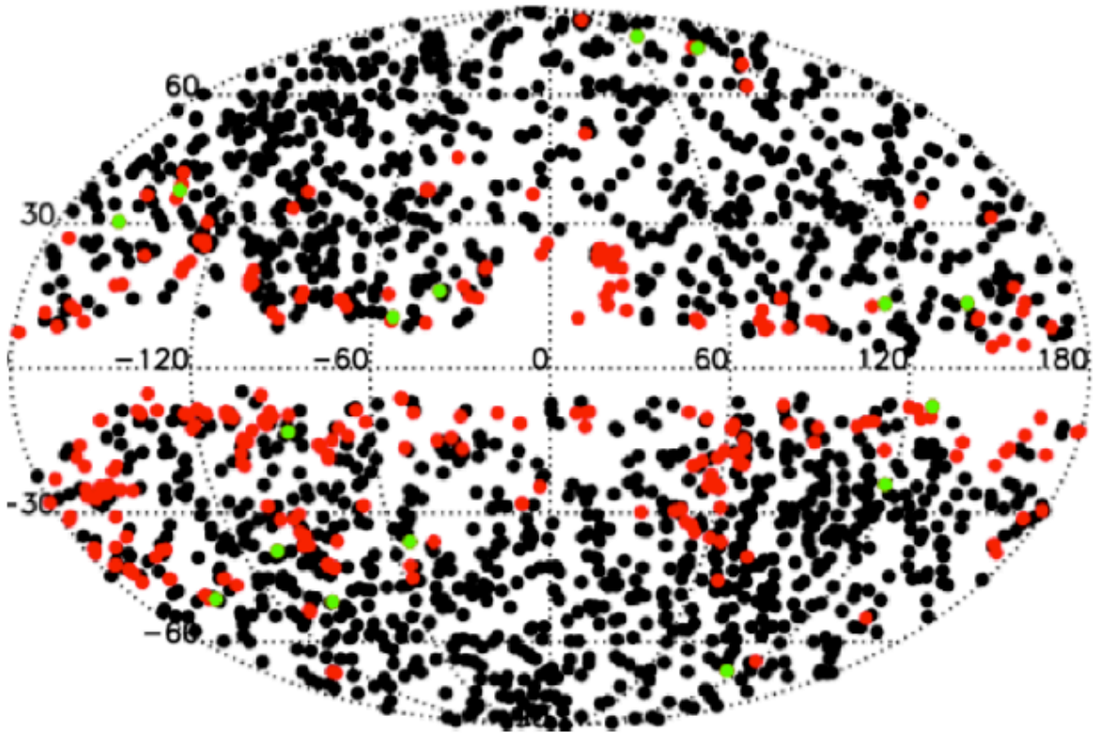

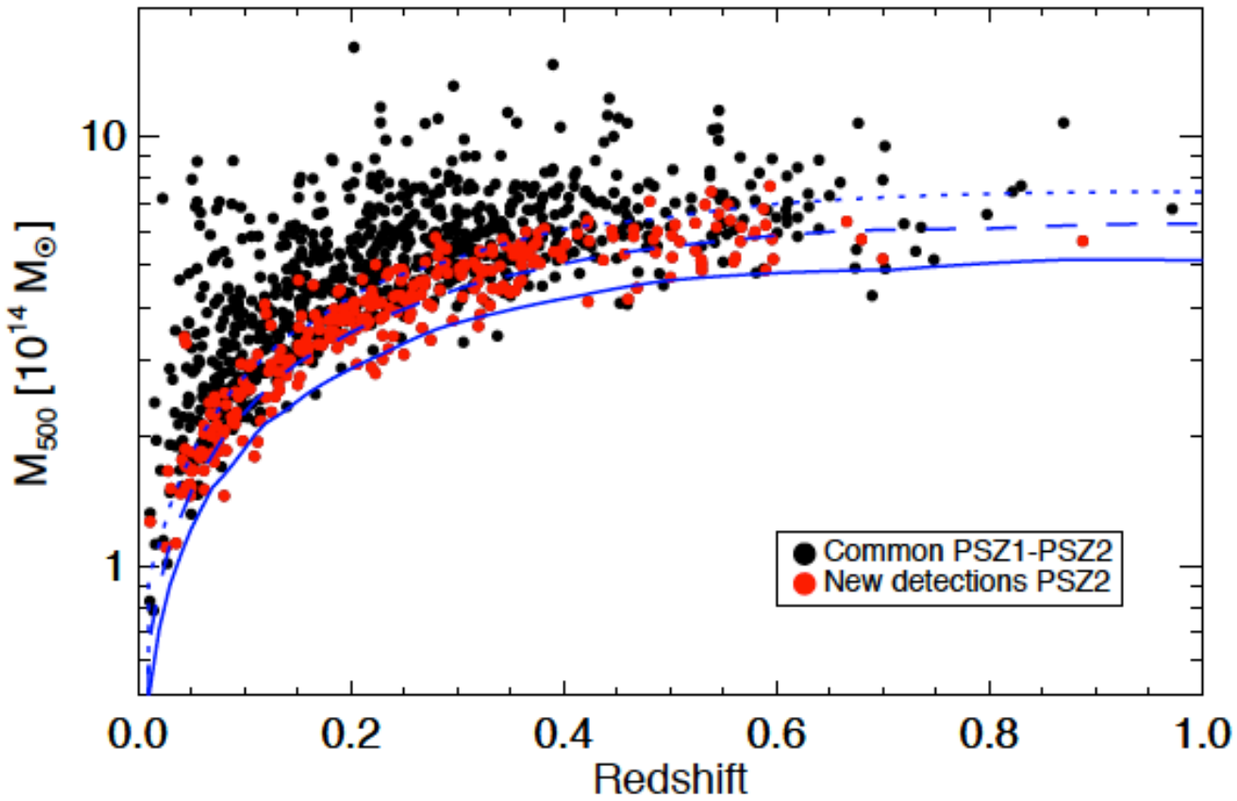

The ~1200 clusters from the Planck catalog in 2015 (PSZ-2).

These might very well represent *all* the massive clusters in the universe (barring those behind our Galaxy).

Counting clusters for cosmology

Mass function describes number of clusters of mass M per unit comoving volume

★ changing cosmological parameters affects:
- shape of MF at z=0
- evolution of MF with redshift

Obtain cosmological constraints by counting n(M) for clusters at different z

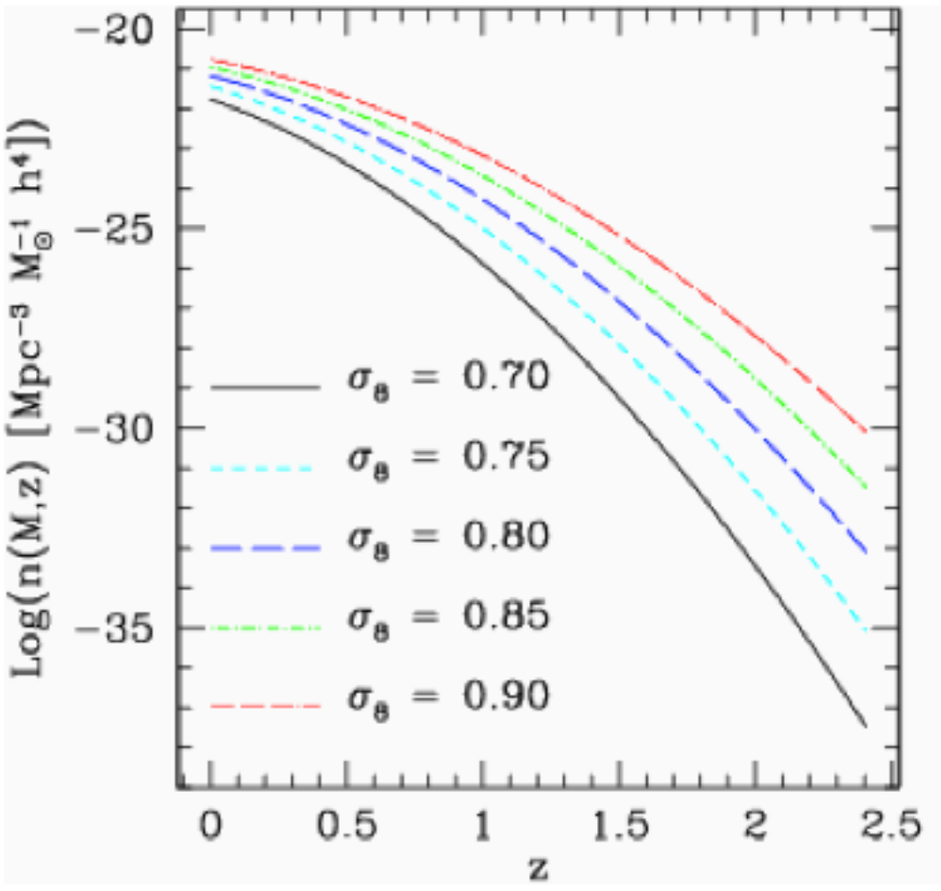

Fedeli et al, (2008, A&A, 486)

Structure growth & cluster count

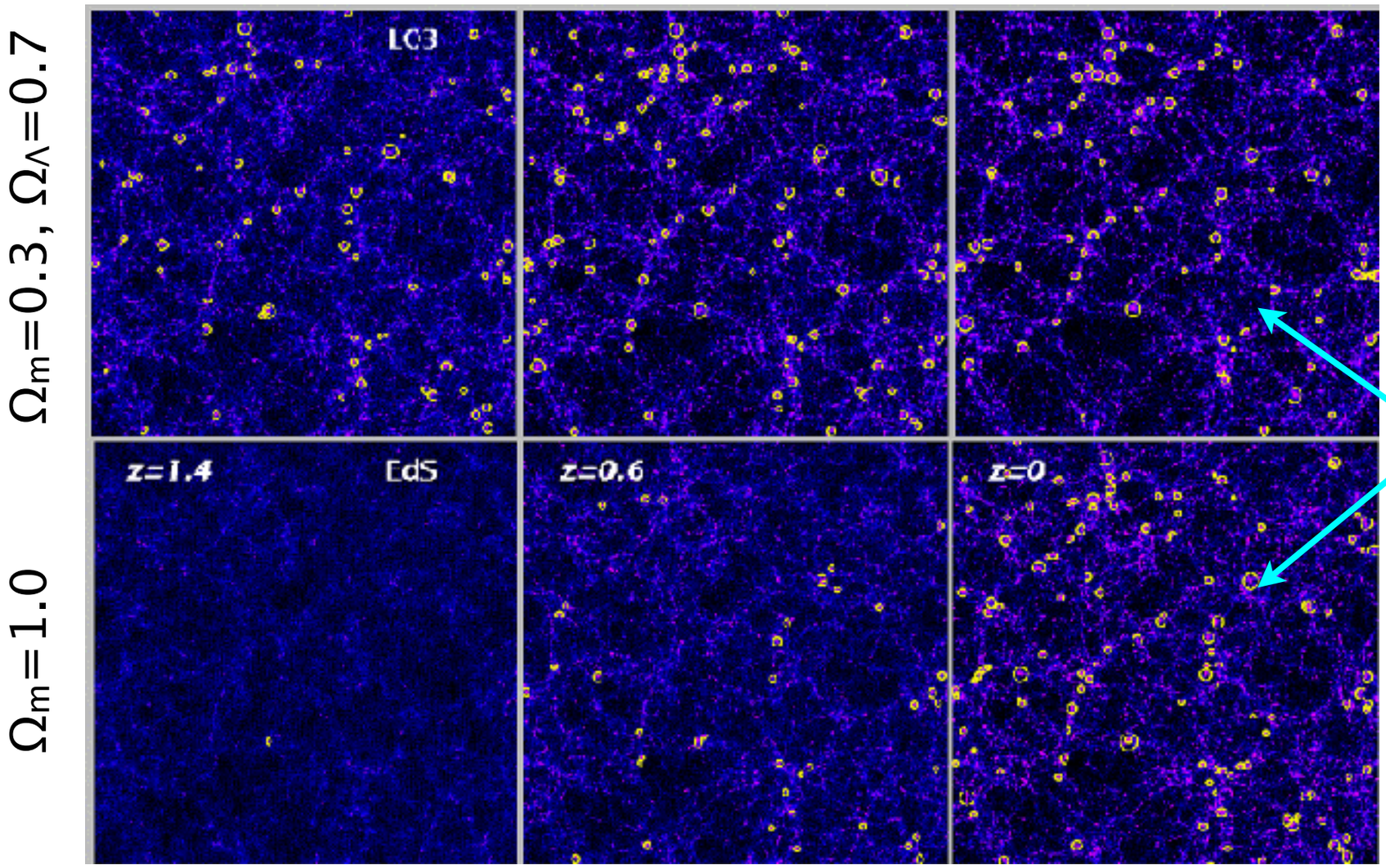

Borgani & Guzzo, Nature, 2001

Example showing the role of galaxy clusters in tracing the cosmic evolution, in particular dark matter and dark energy contents.

Planck cluster cosmology results

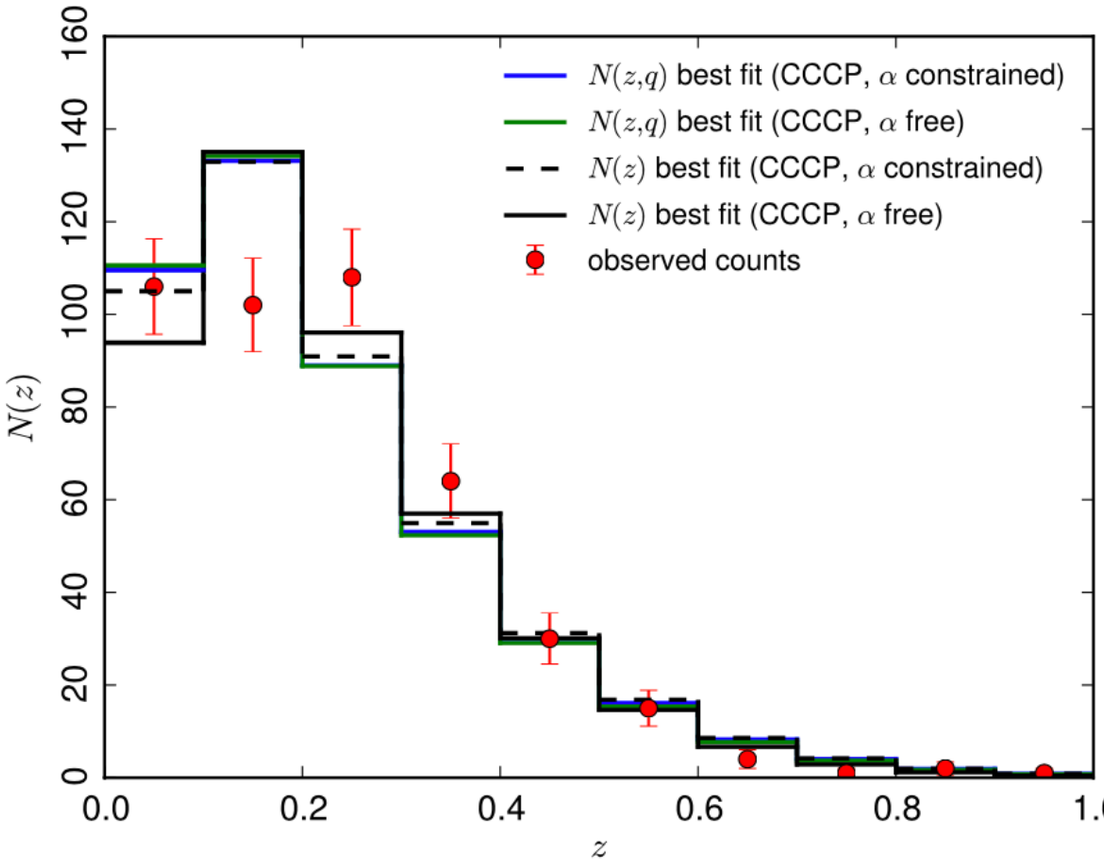

Redshift distribution of the Planck clusters and four different modelling scenarios (Planck+2015)

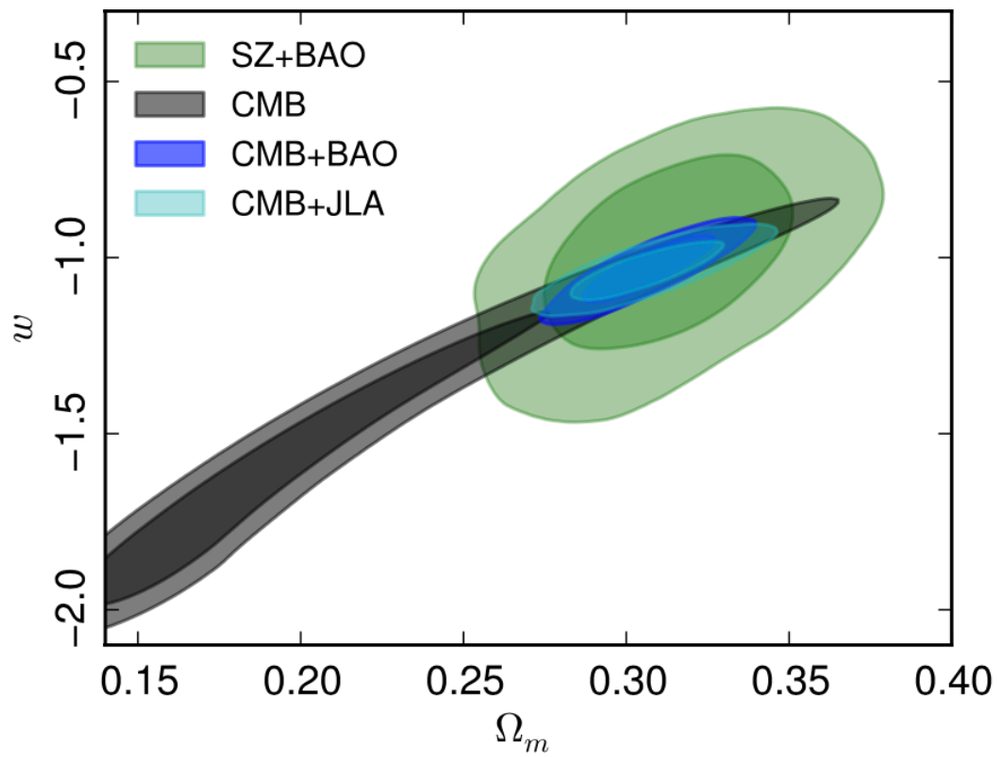

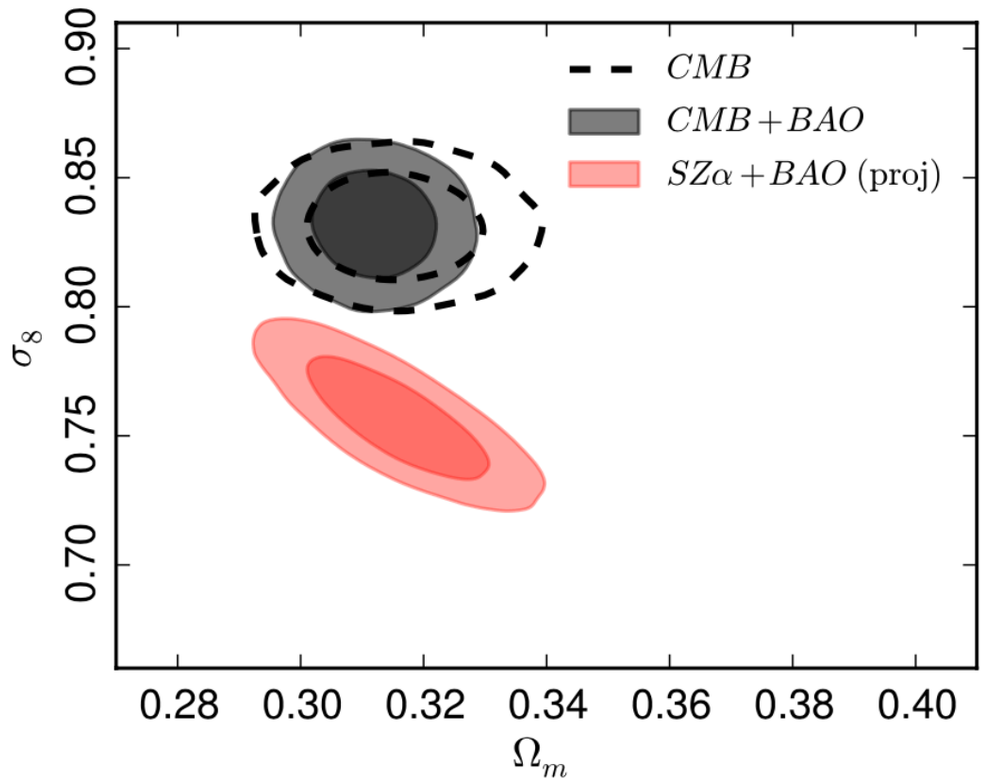

The discrepancy between the σ_8 values, as derived from CMB and SZ-count data, has been attributed to a discrepancy in cluster mass modelling and since been partially resolved.

Planck cluster examples

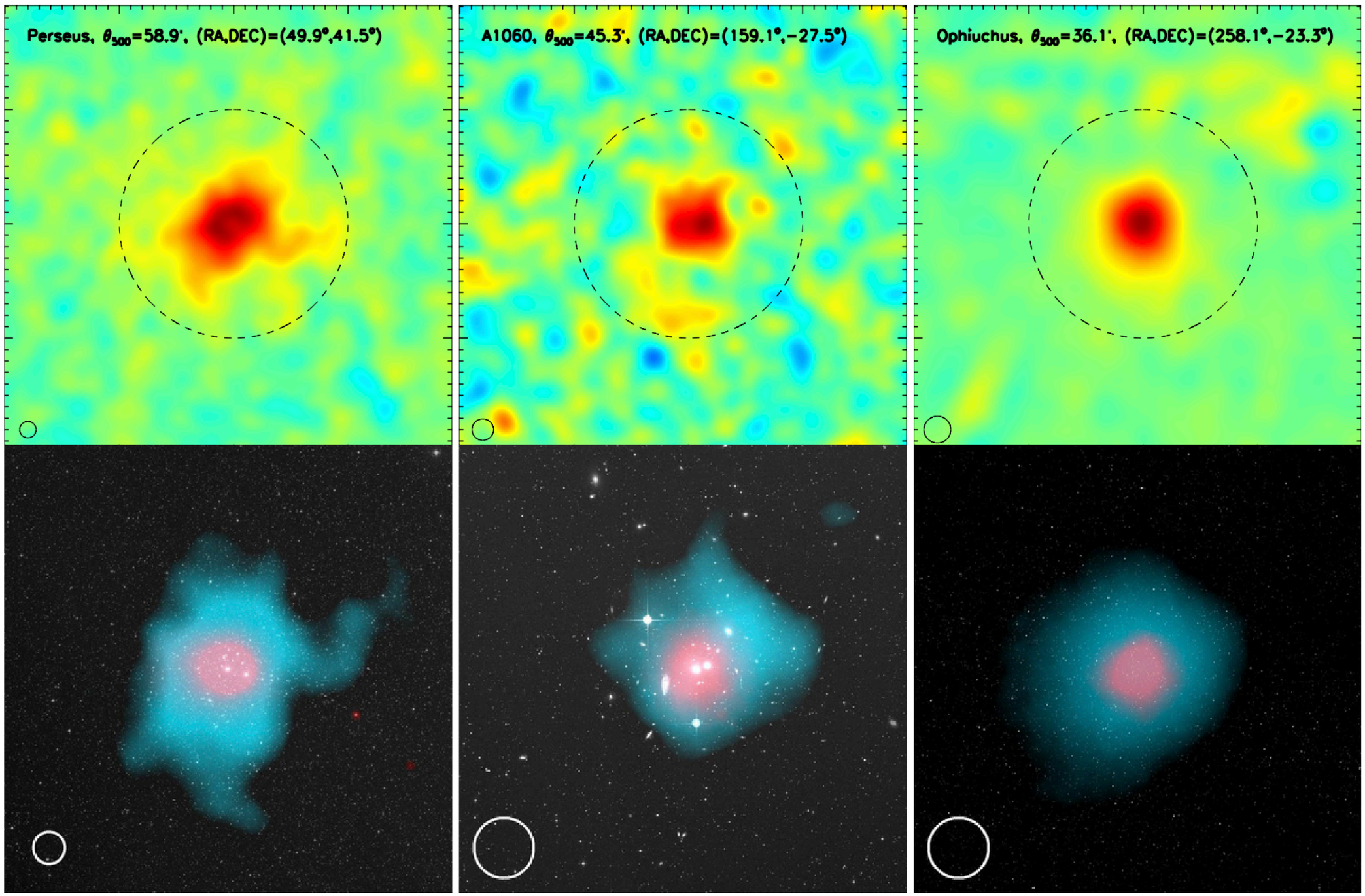

Bottom panel: composite images of the optical (DSS, white), X-ray (ROSAT, pink) and SZ signal (*Planck*, blue).

The Intra-Cluster Medium (ICM)

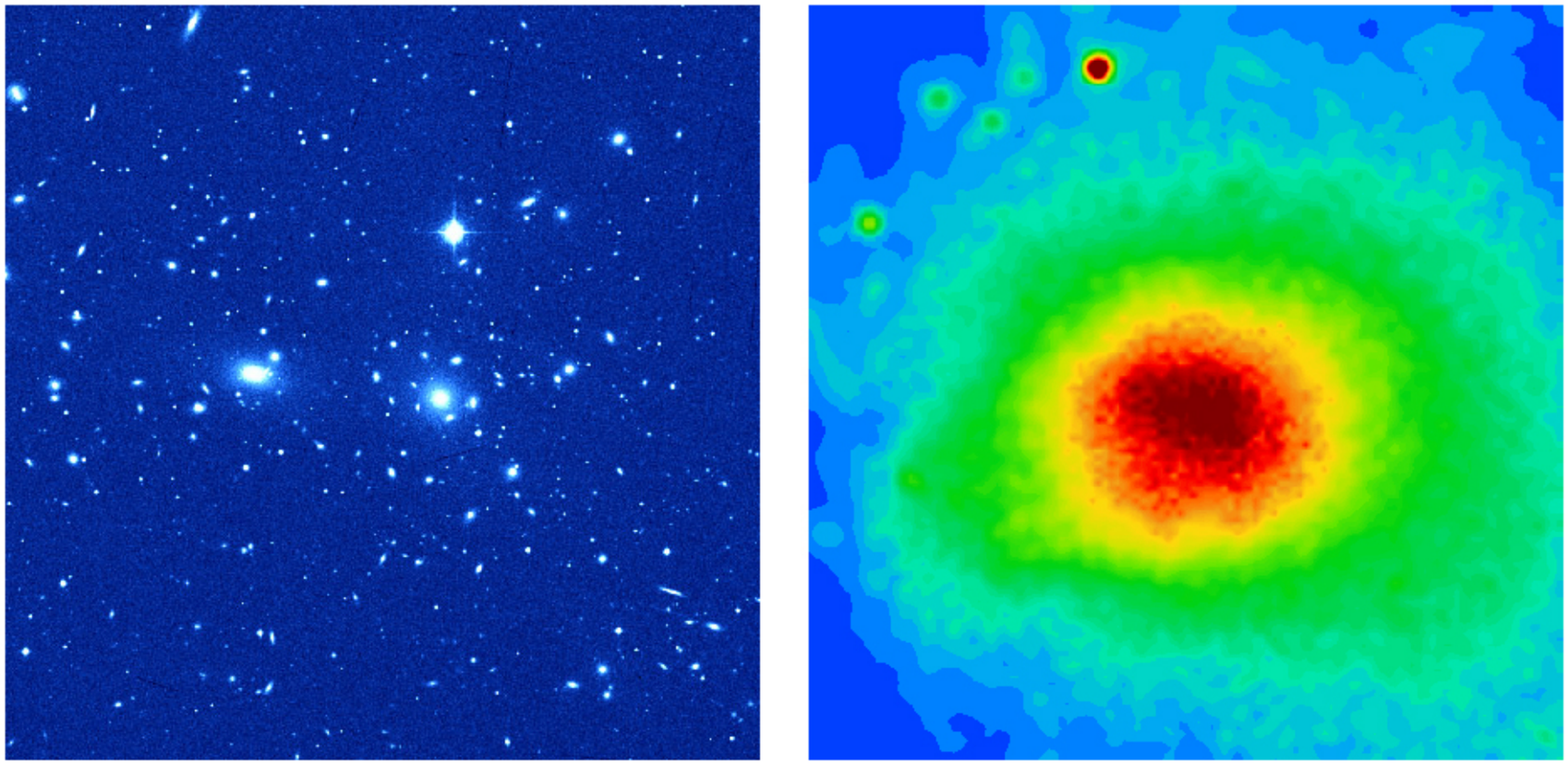

- Most of the observable mass (baryons) in galaxy clusters is in the form of hot intracluster plasma
- Temperature up to T ~ 10^8 K ~ 10 keV, electron density n_e ~ 10^{-3} cm^{-3}
- Mostly H, He, but with traces of heavy elements (O, Fe, ..)
- Mainly emits photons in X-rays (bremsstrahlung), but also radio (synchrotron) and gamma rays (p-p collision)
- Causes the Sunyaev-Zeldovich (SZ) effect by inverse Compton scattering of the background CMB photons

Y_{SZ}: A good proxy for cluster mass

$$Y \equiv \int_\Omega y\, d\Omega = \frac{1}{D_A^2}\left(\frac{k_B \sigma_T}{m_e c^2}\right) \int_0^\infty dl \int_A n_e T_e\, dA,$$

$$YD_A^2 \propto T_e \int n_e\, dV = M_{\rm gas} T_e = f_{\rm gas} M_{\rm tot} T_e.$$

$$YD_A^2 \propto f_{\rm gas} T_e^{5/2}$$
$$YD_A^2 \propto f_{\rm gas} M_{\rm tot}^{5/3}$$
$$YD_A^2 \propto f_{\rm gas}^{-2/3} M_{\rm gas}^{5/3}$$

Planck collaboration (2011)

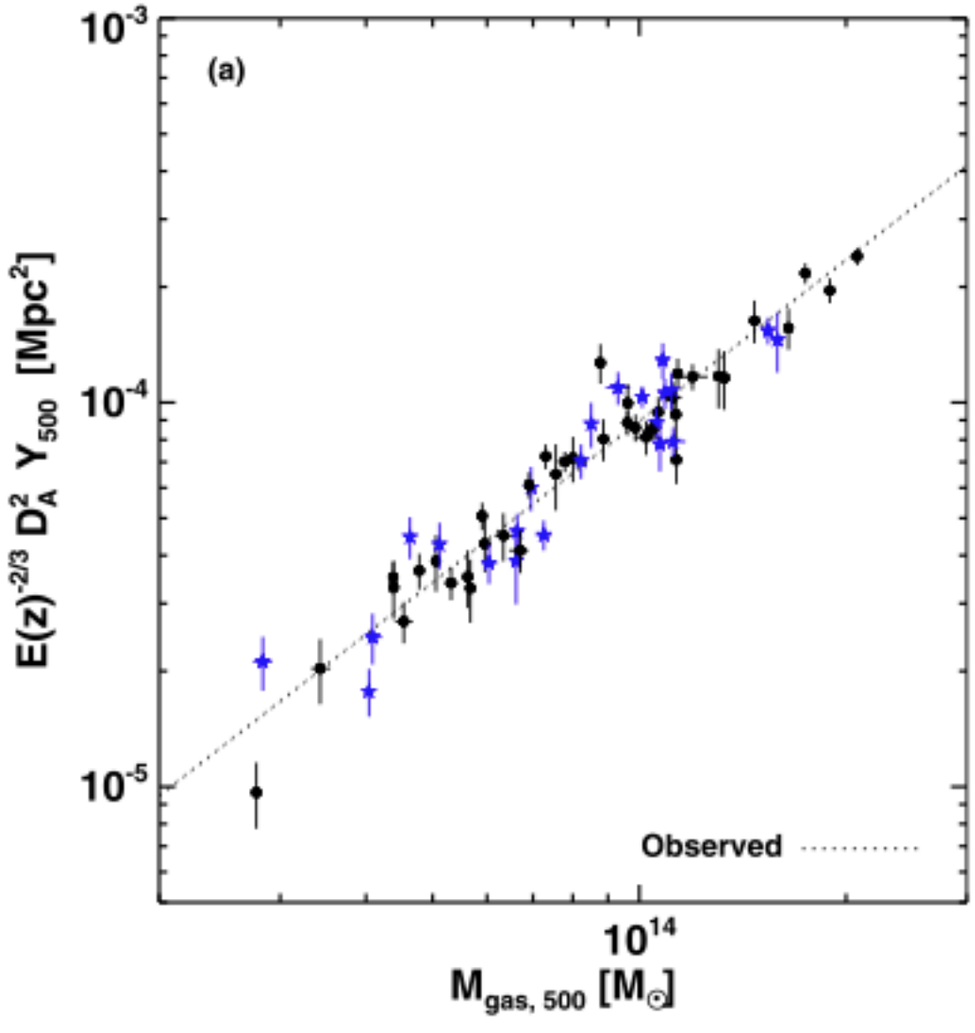

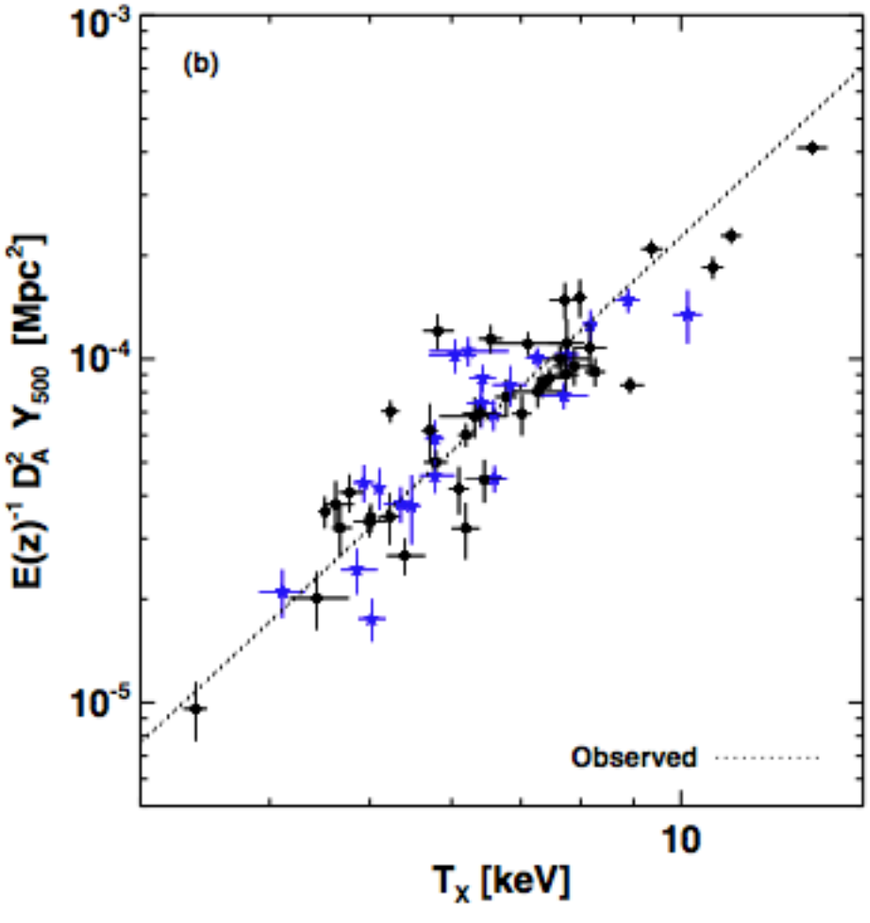

Pressure profile from SZ measurements

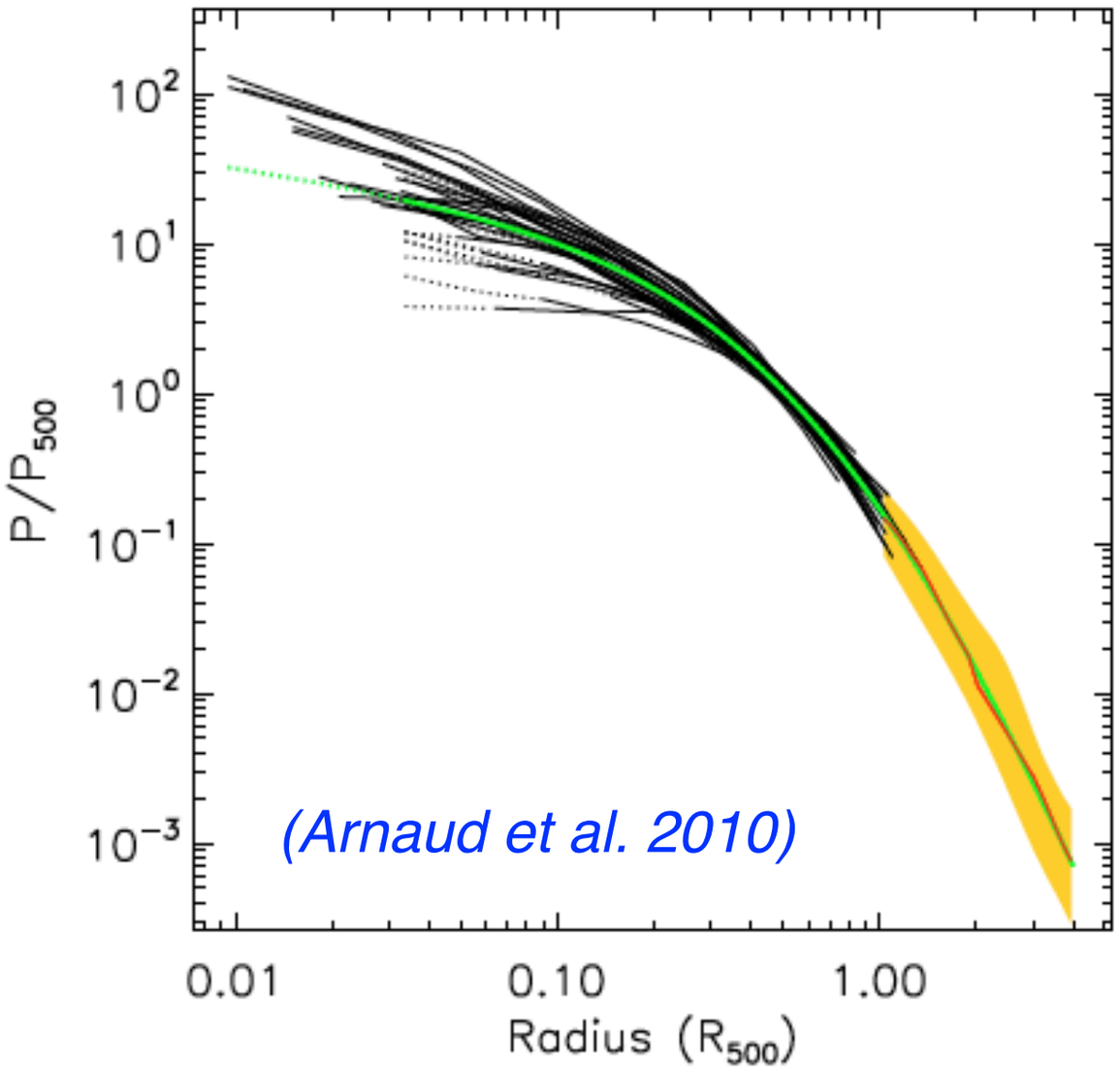

Fig. 8. GNFW model of the universal pressure profile (green line). It is derived by fitting the observed average scaled profile in the radial range [0.03–1] R_{500}, combined with the average simulation profile beyond R_{500} (red line). Black lines: REXCESS profiles. Orange area: dispersion around the average simulation profile.

Since the thermal SZ signal is proportional to the line-of-sight integral of pressure, deprojecting the SZ measurement gives directly the ICM pressure profile.

Generalized NFW (GNFW) model for ICM pressure was proposed by Nagai et al. (2007), Arnaud et al. (2010)

$$\mathbb{p}(x) = \frac{P_0}{(c_{500}x)^\gamma \left[1 + (c_{500}x)^\alpha\right]^{(\beta-\gamma)/\alpha}}$$

$$P(r) = P_{500} \left[\frac{M_{500}}{3 \times 10^{14}\, h_{70}^{-1}\, M_\odot}\right]^{\alpha_P + \alpha'_P(x)} \mathbb{p}\,(x)$$

Integrated SZ signal is estimated from the models by volume-integrating the pressure

$$Y_{\rm sph}(R) = \frac{\sigma_T}{m_e c^2} \int_0^R 4\pi P(r) r^2 {\rm d}r$$

Joint SZ/X-ray modelling

$$\text{X-ray} \sim n_e^2 \Lambda(T_e)$$

$$\text{SZE} \sim n_e T_e$$

SZ effect (thermal) and the X-ray emission probes the same intracluster plasma, but with different n_e and T_e dependencies. Thus, combining SZ and X-ray data, information on these two important quantities can be obtained.

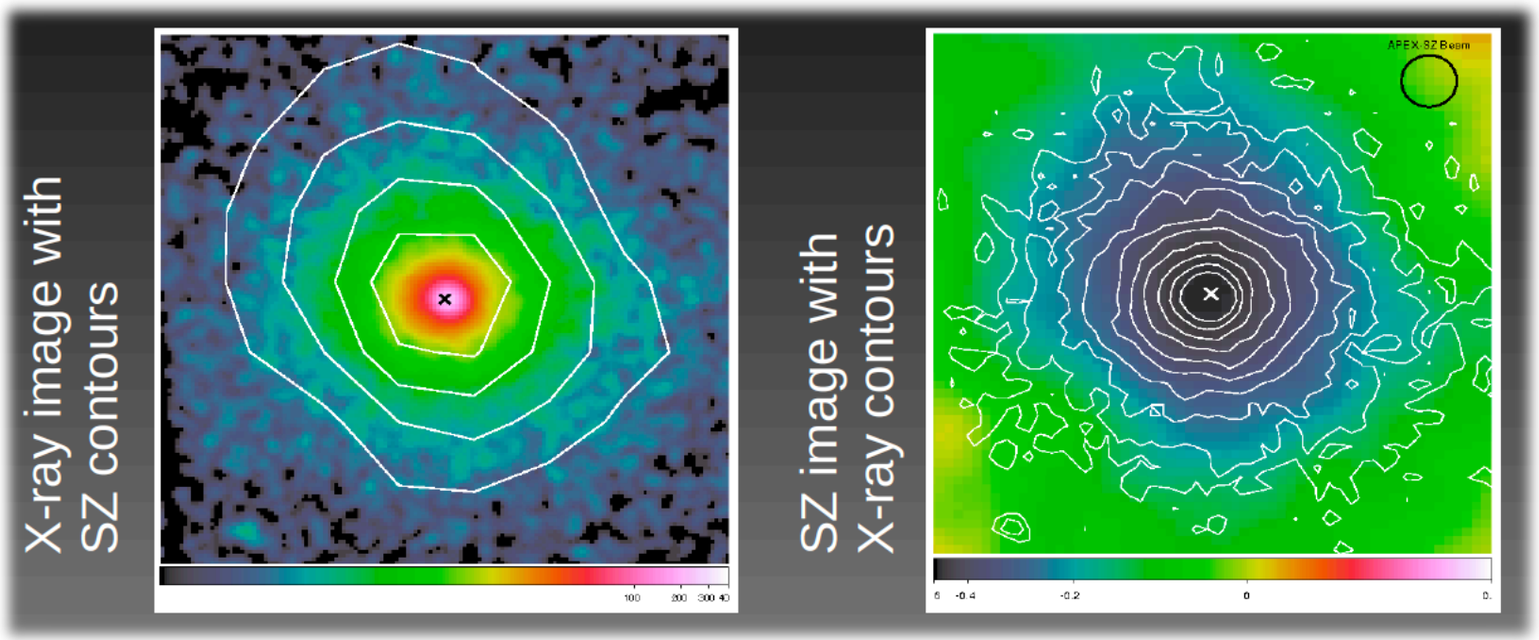

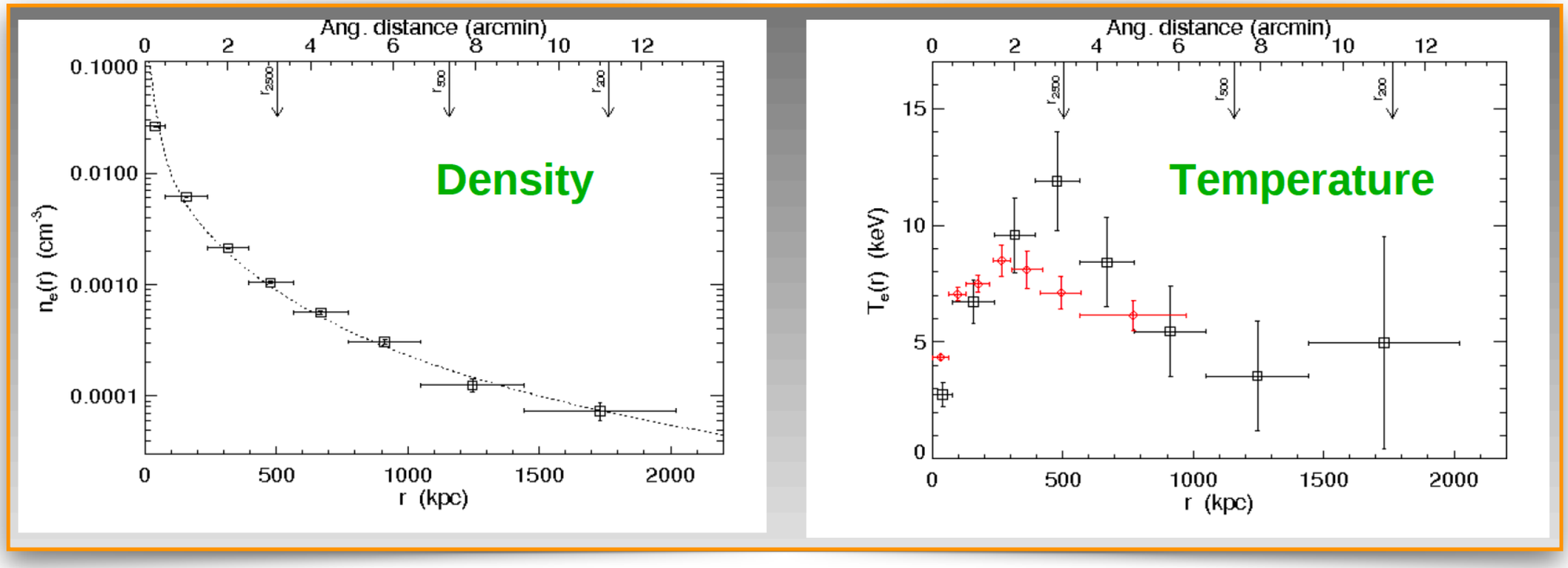

Joint SZ/X-ray modelling of H_0

One can solve for the angular diameter distance by eliminating n_{e0} (noting that $n_{\rm H} = n_e \mu_e / \mu_{\rm H}$, where $n_j \equiv \rho / \mu_j m_p$ for species j), yielding

$$D_{\rm A} = \frac{(\Delta T_0)^2}{S_{\rm X0}} \left(\frac{m_e c^2}{k_{\rm B} T_{e0}} \right)^2 \frac{\Lambda_{e{\rm H}0} \mu_e / \mu_{\rm H}}{4\pi^{3/2} f^2_{(x,T_e)} T^2_{\rm CMB} \sigma^2_{\rm T} (1+z)^4} \frac{1}{\theta_c} \times \left[\frac{\Gamma(3\beta/2)}{\Gamma(3\beta/2 - 1/2)} \right]^2 \frac{\Gamma(3\beta - 1/2)}{\Gamma(3\beta)} ,$$

where $\Gamma(x)$ is the gamma function. Similarly, one can eliminate $D_{\rm A}$ instead and solve for the central density n_{e0}.

Since both X-ray and (thermal) SZ signal depends on the electron density, one can eliminate the n_e (and assume a value of T_e), which gives the angular diameter distance of a galaxy cluster as a ratio of the form $(SZ)^2/X$, from which the value of H_0 can be derived (see expression on left).

From Reese et al. (2002)

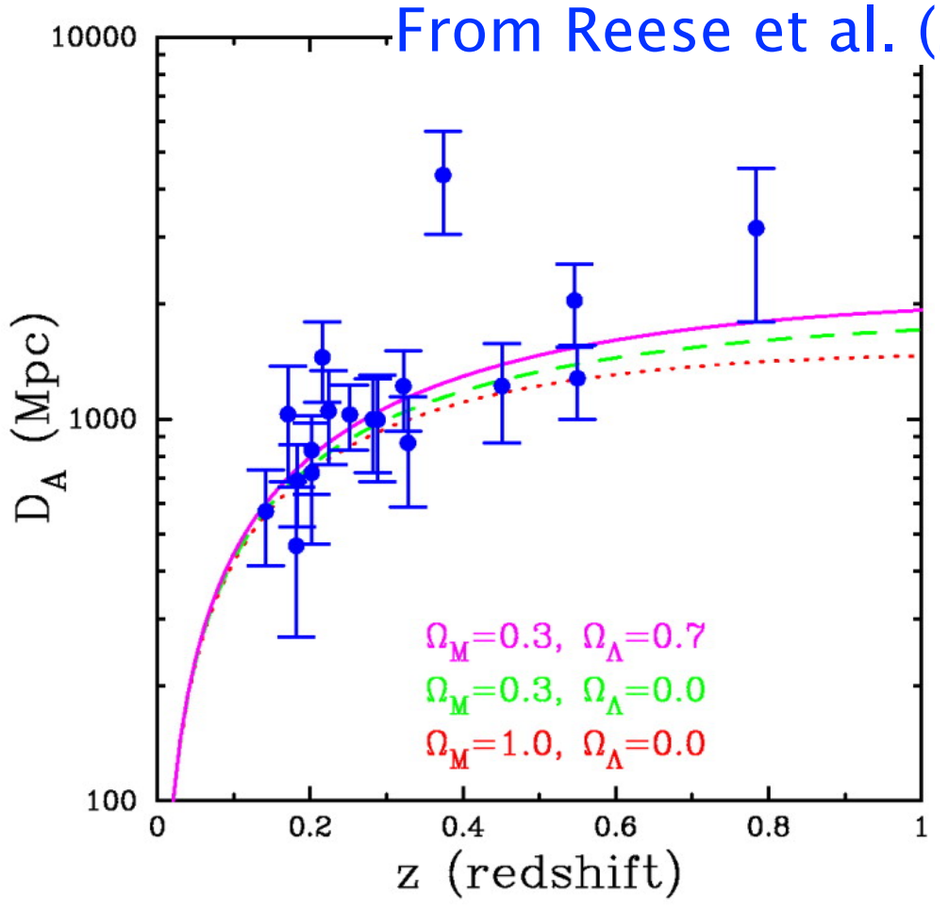

BONAMENTE ET AL. 2006

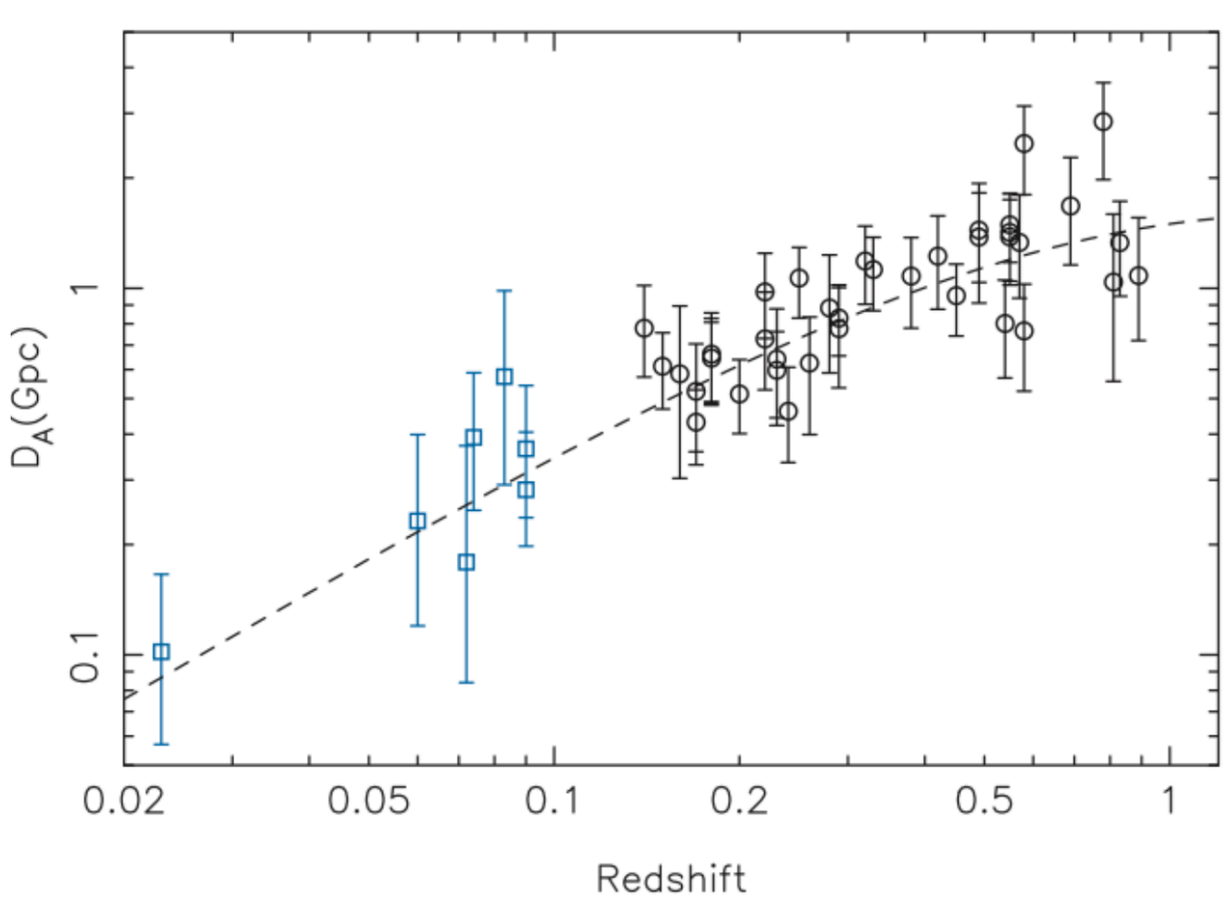

Measurement of ICM temperature from rSZ

Current best measurement with *Planck* data, stacking ~700 clusters

$$k_B \langle T_{SZ} \rangle = 4.4^{+2.1}_{-2.0}\,\mathrm{keV}$$

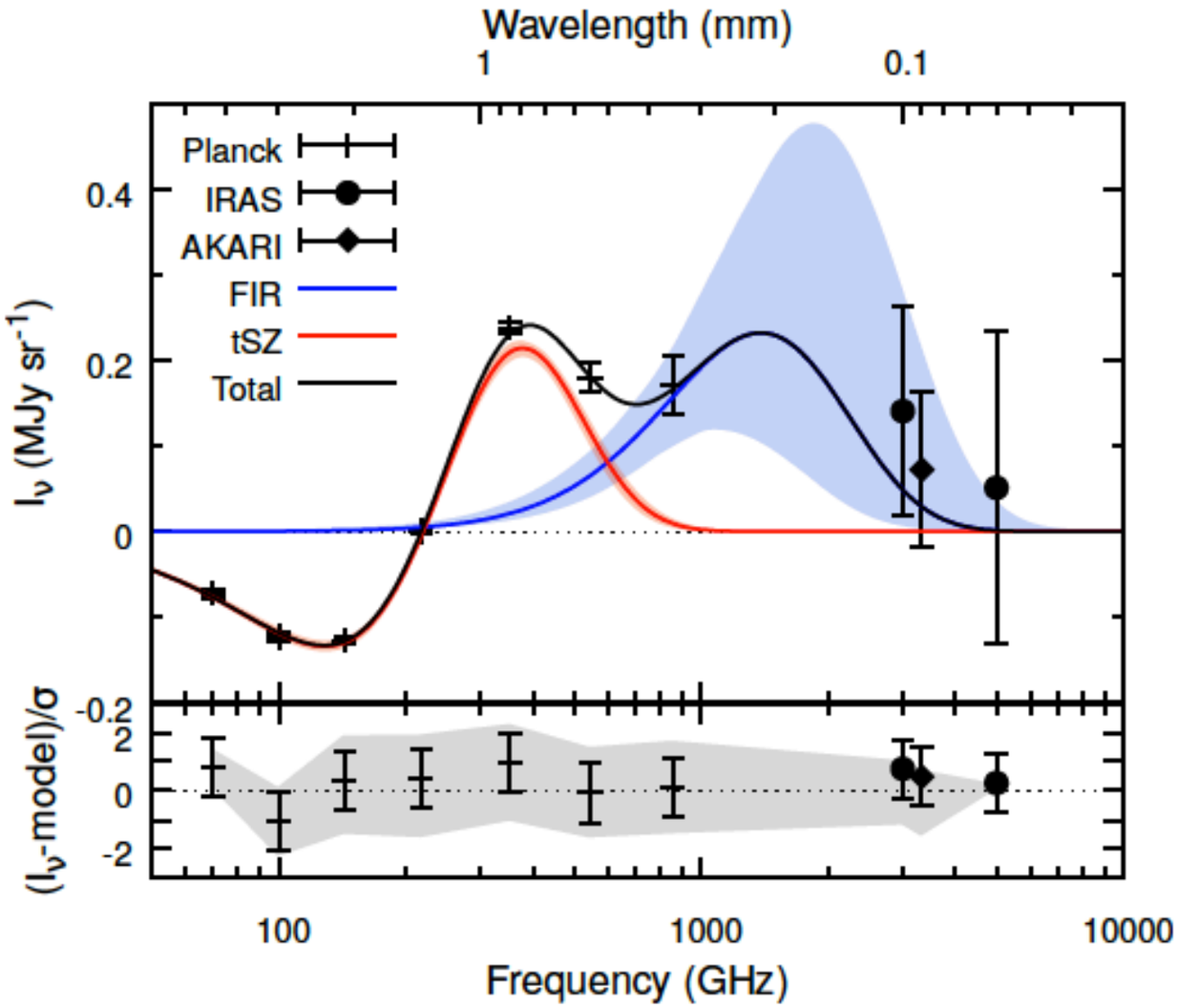

Erler, Basu et al. (2018)

Measurement in a single, massive cluster RXC J1347

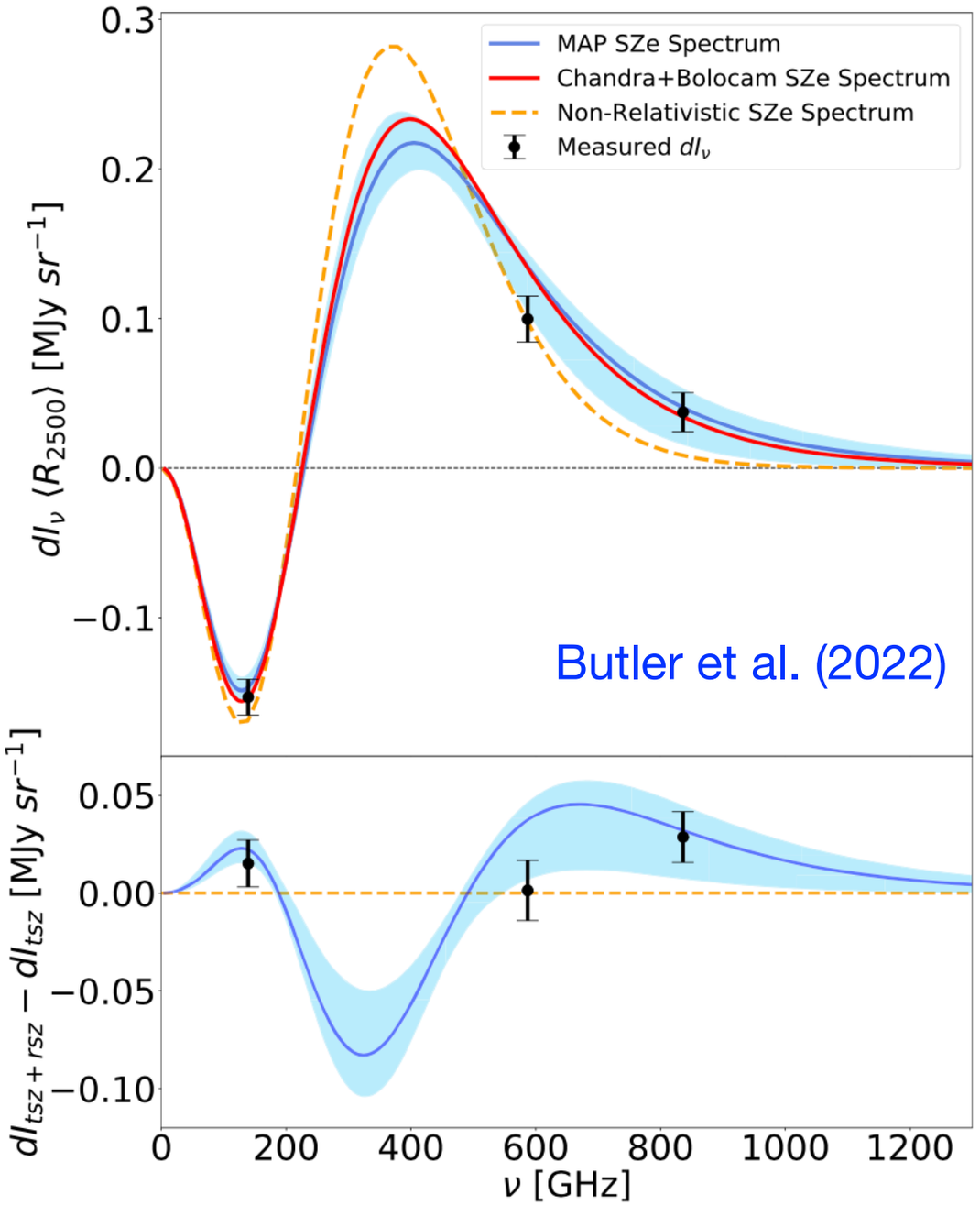

Butler et al. (2022)

$\langle T_{sz} \rangle_{2500} = 12.3\,\mathrm{keV}$ with a 68% credible interval
$5.8 < \langle T_{sz} \rangle_{2500} < 20.5\,\mathrm{keV}$

Measurement of the SZ zero-crossing

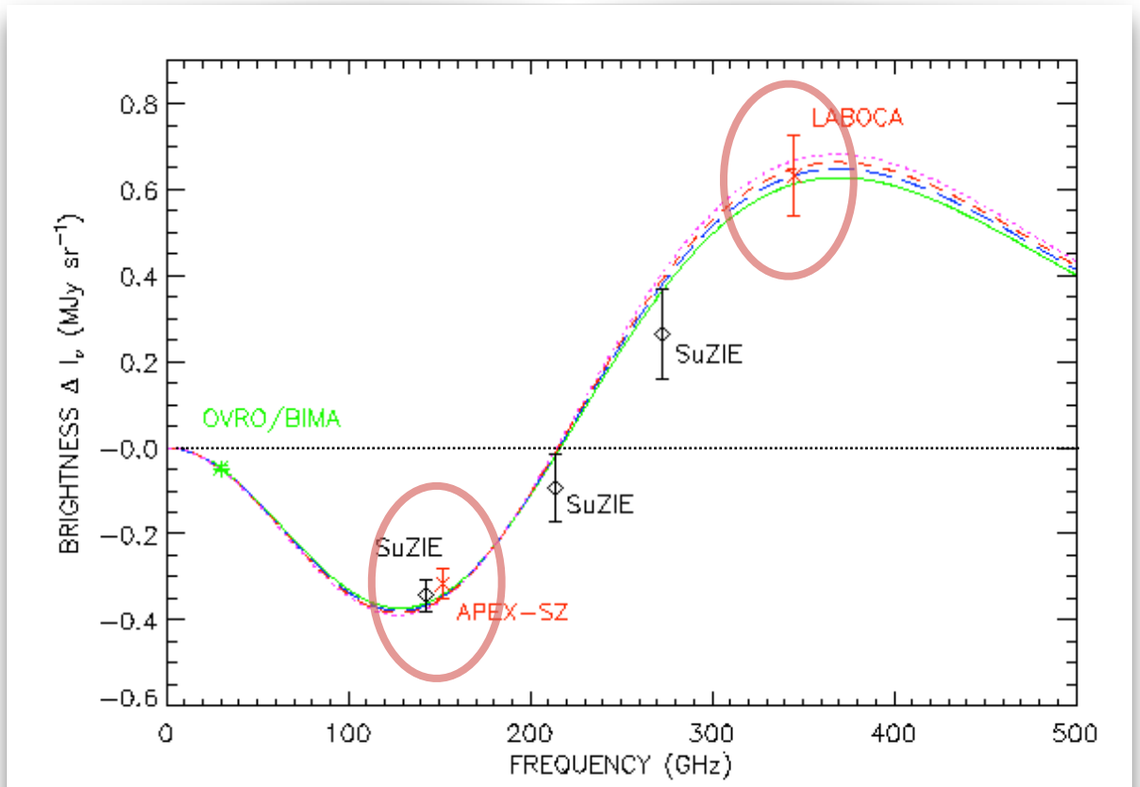

Nord et al. (2009), using our own APEX-SZ and LABOCA measurements of the SZ effect.

We obtained $v_r = -140 \pm 460$ km/s from the spectral fitting, assuming a temperature of 10.4 ± 1.4 keV (from SZ/X-ray modelling)

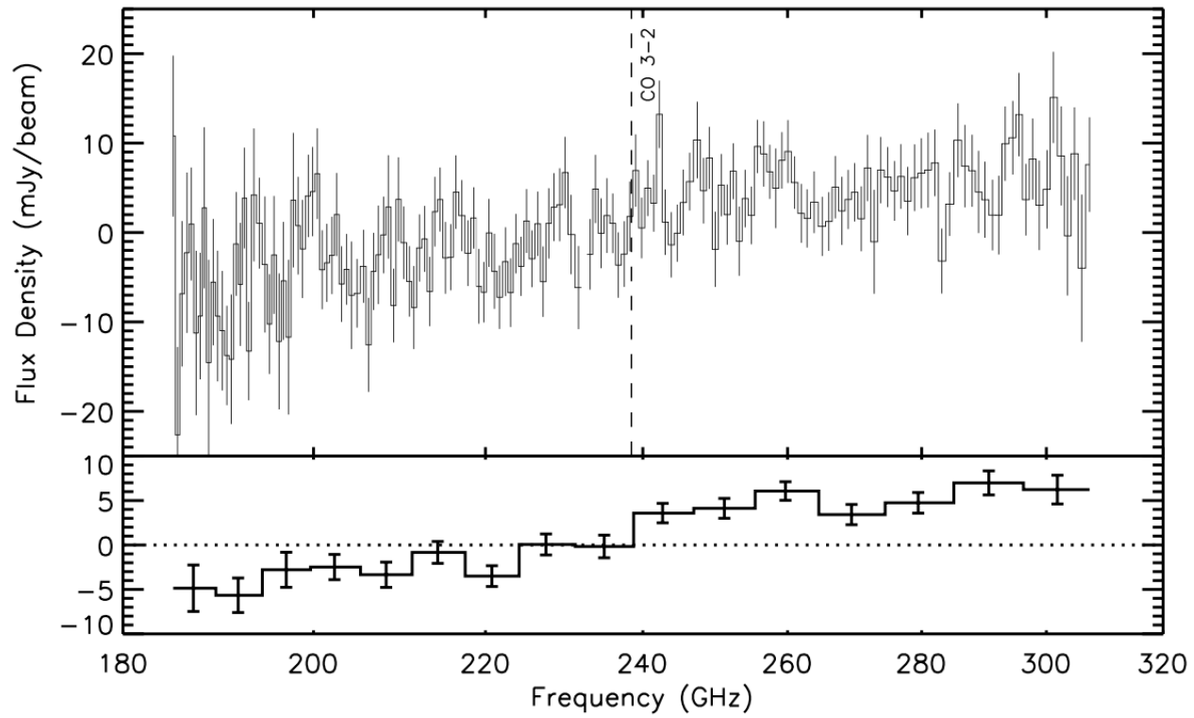

Zemcov et al. (2012) for the massive cluster RXCJ1347, finding $\nu_0 = 225.8 \pm 3.7$ GHz.

Forecasts for the CCAT-prime spectrometer

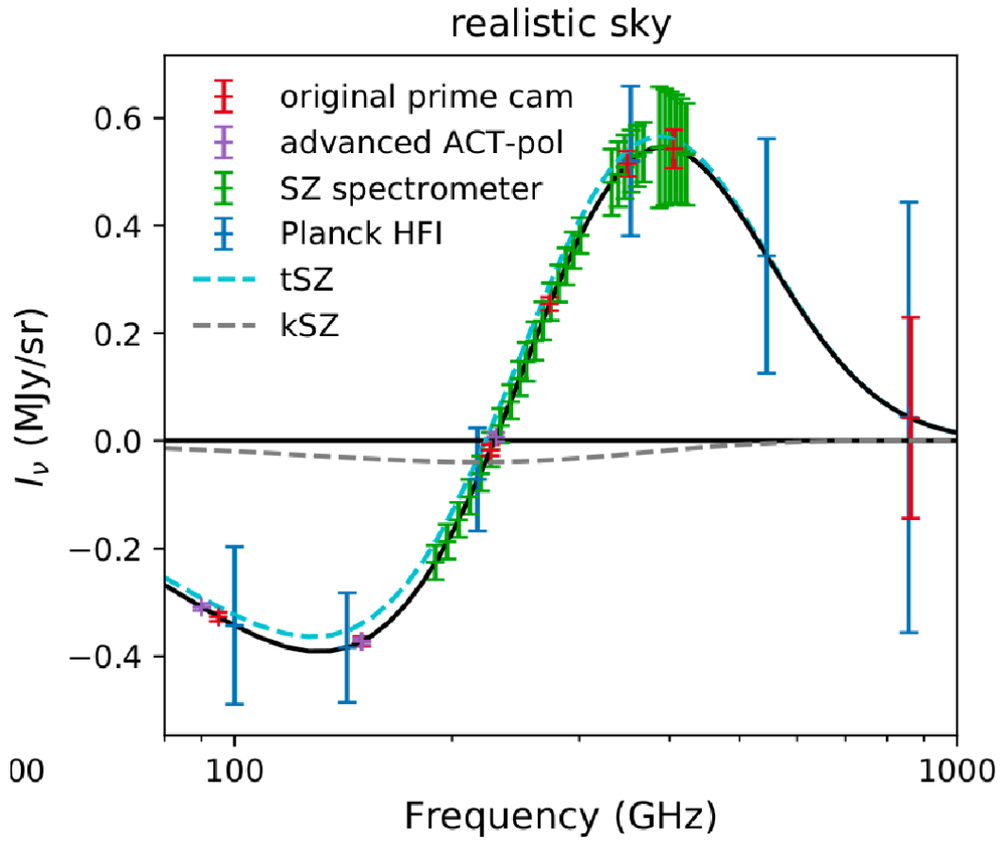

SZ measurements of the WHIM

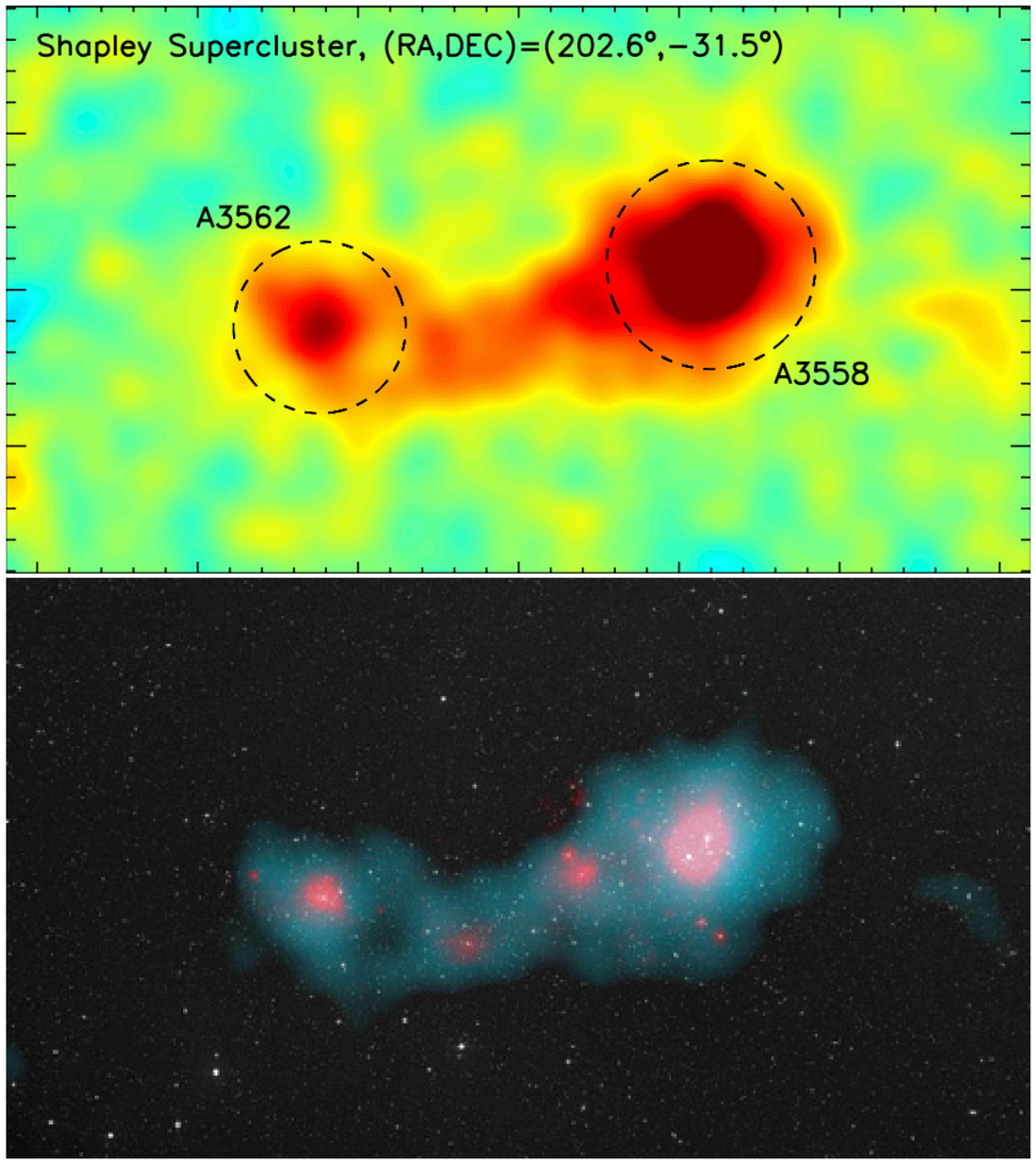

Planck measurement of the Shapley supercluster. Upper panel: tSZ measurement. Lower panel: composite image of optical (white), X-ray (pink), and tSZ (blue).

Most of the baryons in the local universe are in a warm-hot phase in the cosmic filaments, not bound to galaxy clusters. This phase is called WHIM (Warm-Hot Intergalactic Medium). Measuring it is key to understanding the cosmic evolution of baryons.

Since SZ signal depends linearly on density, it is a perfect tool to observe ionized plasma from low density environments, including WHIM.

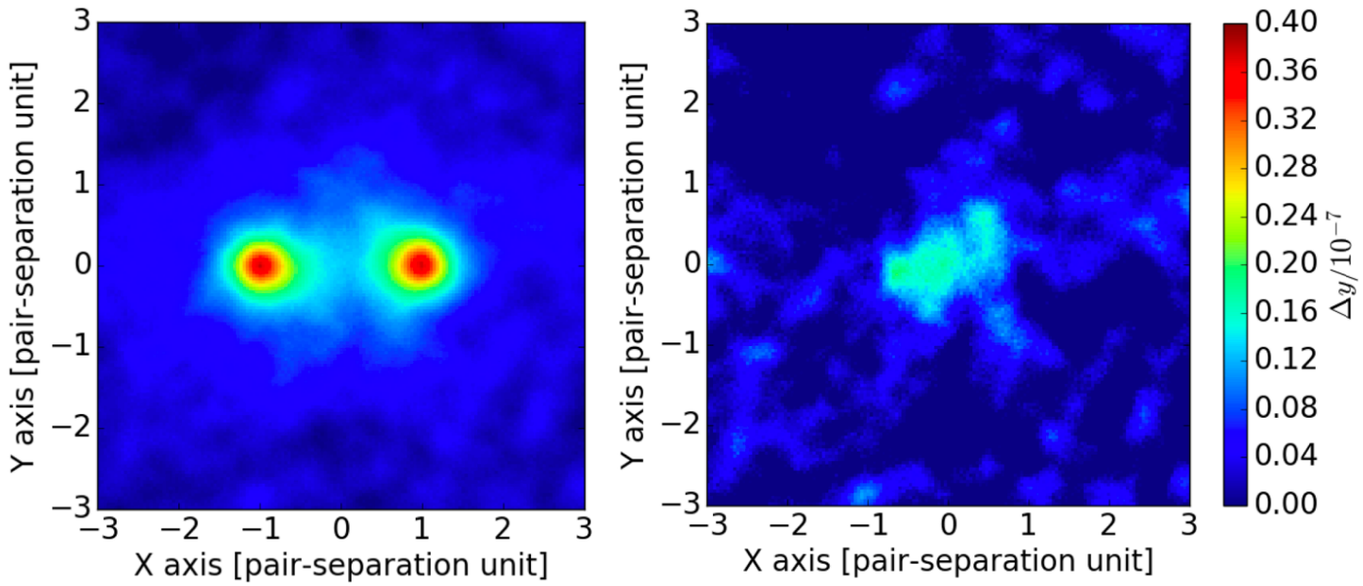

Stacking of the SZ signal as halo pairs (galaxy pairs) and subtracting the halo component to get to the WHIm residual. From Tanimura et al. (2019).

Questions?

Feel free to email me or ask questions in our eCampus Forum